

DATS 6203 Final Project Group-4 Report

Maeshal Hijazi, Yifu Li, and Jinshun Su

December 8, 2020

1 Introduction

This project investigates the effective utilization of the Autoencoder (AE) neural network model for online identification of the distribution system (DS) topology based on a large amount of real-time phasor measurement units (PMUs) detection data. In subsection 1.1, we provide background information on several recent high-impact low-probability (HILP) events that led to prolonged electricity outages and highlight the criticality of DS resiliency and reliability. In subsection 1.2, we discuss the current practice for DS topology identification through PMUs data. Eventually, the report outline is presented in subsection 1.3.

1.1 Background

In recent years, there has been an increase in the frequency and magnitude of HILP events—which, according to recent statistics [1], have resulted in excessive equipment damages, prolonged electricity outages, significant economic losses, and disruptions in our modern society. In the USA in particular, a total of seventy weather-driven disasters occurred from 2015 to 2019 and resulted in billions of dollars of costs [2]. Seven major blackouts in the U.S. history lasted between 10 and 50 hours, with the associated costs exponentially increasing as the duration of the outage increases. Example events with major electricity outages are: 1) the 2017 Hurricane Harvey causing substantial electricity outages (around 10,000 MW) and leaving more than 291,000 people without power; 2) the Hurricane Sandy in 2012 resulting in 10 percent of customers in New York and New Jersey without power for 10 days, \$14 to \$26 billion economic losses, and 50 deaths due to the sustained outage of electricity [1].

The power system serves as the backbone for lifeline networks and drives a myriad of interdependent systems and mission-critical services, such as water, communication, transportation, health, military, and government sectors and services. A bulk power system mainly consists of three hierarchical levels including generation system, transmission system, and DS. The generation system owns different types of power plants to produce electric power, mostly located far away from the demand centers. The gener-

ated electricity is transmitted over hundreds of miles through the transmission system from distant power plants to demand centers. In each demand center, a substation is located facilitating the transfer of electricity from the transmission system to the DS, the DS then brings the electricity to individual customers. While all three segments of the bulk power system might be vulnerable to extreme events, the DS provides the last mile electricity connection to the end-consumers and is particularly vulnerable due to its radial topology. Any disruption in the DS may directly and swiftly translate into customer interruptions and power outages. With the increasing frequency and intensity of HILP events, it is primordial to identify and estimate the real-time DS topology following these events, which can contribute to ensure continuous, secure, and reliable supply of electricity to the end-use consumers particularly mission-critical services.

1.2 Current Practice for DS Topology Identification by PMUs

In order to generate and dispatch the power grid stably and safely, especially under a HILP event, system operators need to be informed of the DS topology at all time. With increasing complexity in the DS structure growingly reinforced with heterogenous resources and the increasing demand for electricity needed for an electrified economy, PMUs have been introduced and widely deployed to observe the dynamic performance of the power grid with synchronized measurements. A PMU is a device used measure the magnitude and phase angle of an electrical phasor quantities (e.g., voltage and current) in DS applying a common time source for synchronization [3]. Due to the fact that the time is synchronized by the Global Positioning System (GPS), PMUs are able to capture real-time electrical phasor quantities from multiple remote points on the DS, thereby providing a real-time snapshot of the entire system making it possible to approach wide-area monitoring, protection and control.

Several recent researches [4–6] propose mathematical models for topology identification based on PMUs data. The frameworks of their models assume a DS topology first, and then measure the collected data to compare the features and determine the accuracy of the topology of previously assumed DS. Such strategies are time-consuming, less accurate, and with practical limitations. To overcome the limitations of these math-

ematical models, the study [7] presents a training artificial neural network model to automatically recognize the DS topology and solve complex problems. The learning algorithm of this study is based on a nodal voltage graphical model which only uses data of magnitude and phase angle of system's voltage from PMUs. Comparing with [7], our study employs magnitudes and phase angles of both voltage and current collected by PMUs on our proposed AE model, which can enhance accuracy and robustness of the model for DS topology identification.

1.3 Report Outline

An Autoencoder (AE) is a type of artificial neural network used to learn efficient data coding in an unsupervised manner. It could be used in supervised learning and unsupervised learning. The aim of an AE is to learn a representation (encoding) for a set of data, typically for dimensionality reduction, by training the network to ignore signal "noise" [8].

In this study, the proposed AE for the heatmap classification in the IEEE 34-Node Test Feeder has the following architecture:

The flowchart of the proposed Autoencoder is shown in Figure 2, where the first step is to collect PMU data and normalize them into per-units. Such data with their corresponding topologies are then inputted into the neural network, and the trained network learns to identify distribution grid topology with PMU measurements. The AE used mean squared as the loss function. Finally, we used additional PMU measurements beyond the training set to verify the model accuracy.

This Autoencoder architecture will be used as a building block in the proposed framework that identifies the power distribution network topology in real-time. The relation between the PMU measurements and the AE module will be detailed in the Section 3.

The rest of this report is organized as follows: Section 2 introduces the source of dataset utilized to this project and presents the preprocessing of dataset. Section 3 describes the proposed AE model for DS topology identification. The numerical results and discussions are provided in Section 4, and finally Section 5 concludes the report.

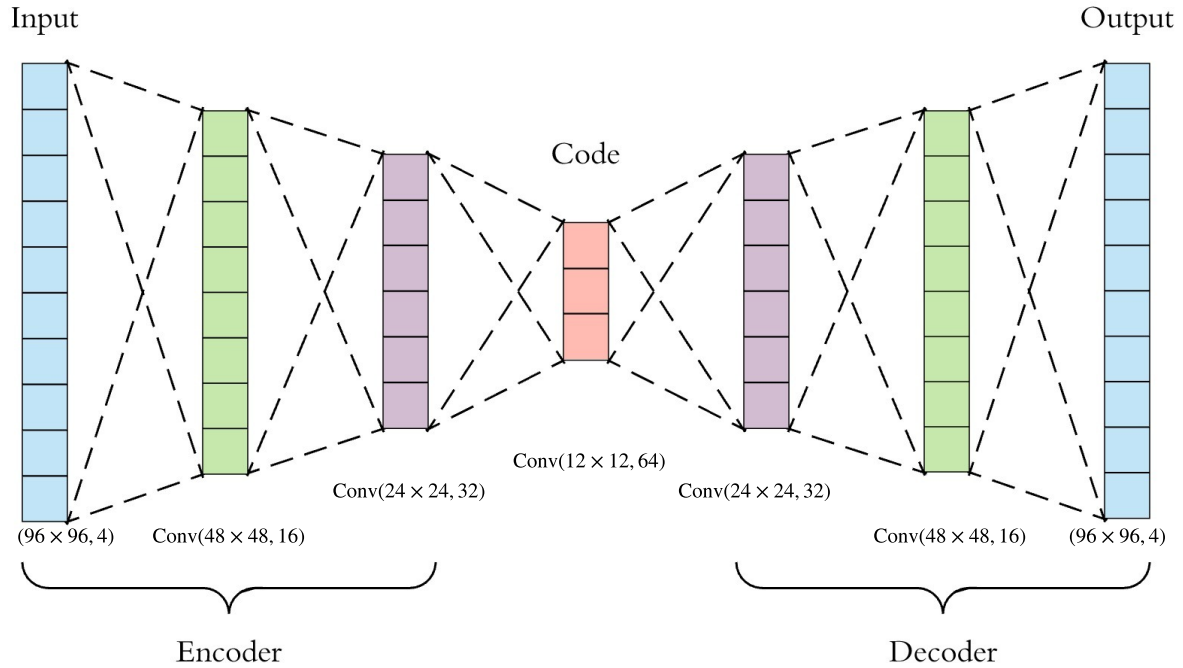


Figure 1: Proposed Autoencoder architecture.

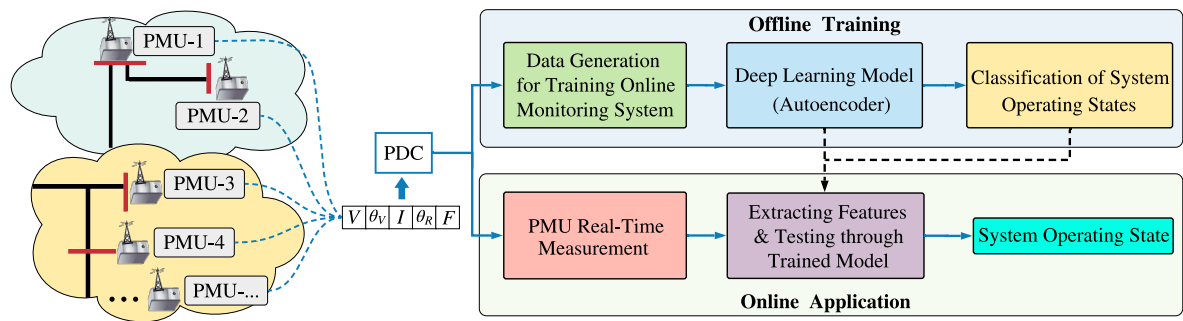


Figure 2: Autoencoder working flowchart.

2 Data Mining

2.1 Dataset Description

The dataset we used in this project is the PMU data which is generated from IEEE-34 node test feeder [9] by Matlab Simulink. This radial power DS is an actual feeder located in Arizona, and its topology is illustrated in **Figure 3**. The detailed information of IEEE-34 node test feeder is presented in Appendix A. Noted that IEEE-34 node test feeder is an unbalanced network, different colors are here used to mark the phasing status. For example, we used pink to mark the line 800-812 as BACN, indicating that it is a three-phase four-wire segment in DS. To gain a full observation of the IEEE-34 node test feeder, we set 33 PMUs on each node expect node 800 (substation bus). We also added 5 breakers (see **Figure 3**: SW1-SW5) in order to generate different network topologies for the AE training dataset. To generate more scenarios under one topology, we marked 5 loads (see **Figure 3**: Load1-Load5), which allows the PMU data could be varying under different realization of the load demand.

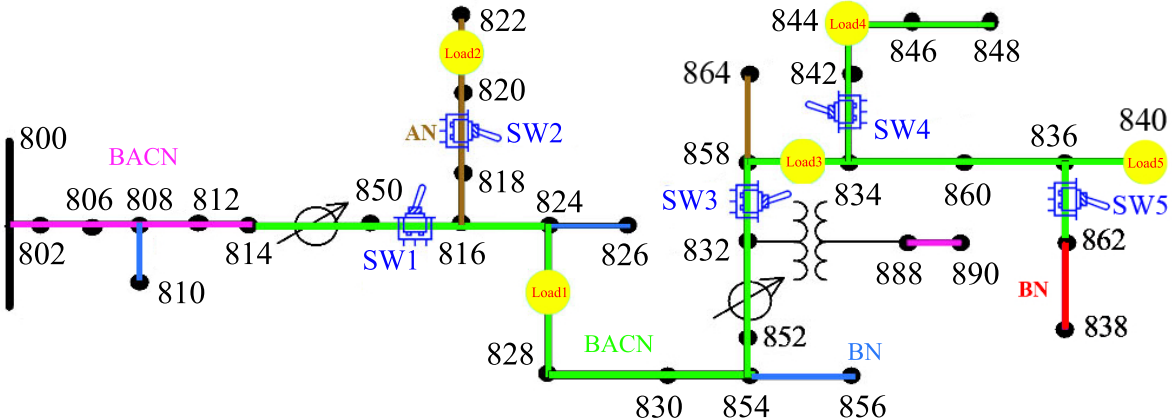


Figure 3: IEEE 34-Node Test Feeder Scenarios.

Upon simulating each scenario in Matlab Simulink environment, the resulting PMU data will characterize a 33 by 12 heatmap matrix which contains three-phase voltage, three-phase voltage angle, three-phase current, and three-phase current angles (see **Figure 4** for a heatmap example). For the nodal measurements that contain single-

phase or two-phase data, we let the remaining entries be zero. We line up the data in a heatmap format into eight groups (8 labels), process the data in each group individually, and finally integrate the information in each group together. A partially connected neural network is dedicated to the processing of these groups of heatmaps.

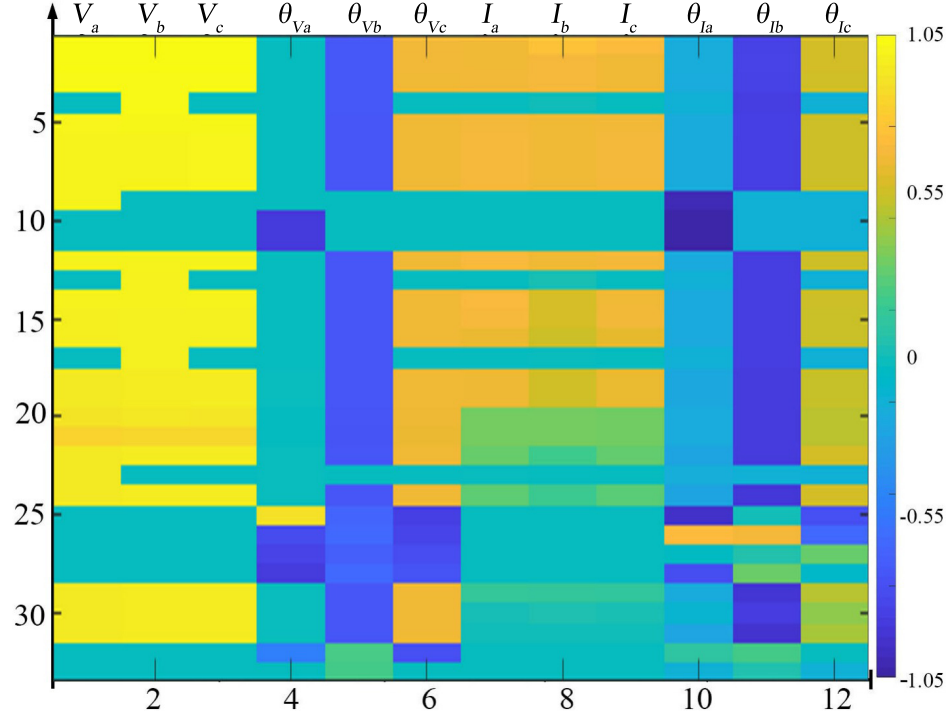


Figure 4: A Heatmap Example of the Generated PMU Measurement Data Sample.

Table 1 shows the general configuration all simulated scenarios, and the exact topologies of different scenarios are illustrated by **Figure 5**.

Take Topology 1 as an example, Breakers SW1 and SW2 are closed (status=1), the rest of Breakers are opened (status=0). For each network topology configuration, we generate different scenarios by adjusting the loads values. To keep the *balance* of training dataset and avoid generating *redundant* training data for the AE model, keen considerations were taken into account in generating different load scenarios. We let the load change amplitude distributed between 95% to 105% of the rated demand at each load point based on different number of served loads: i) Topology 1, only Load 1 and Load 2 are served through the connected distribution line and it is not necessary to adjust the remaining three load points for scenario generation. Assuming each load has 40 possible amplitudes in the constrained range above, the total number of scenarios is found 40^2 (1600) in this case; ii) the network Topology 2, 3 has three loads (i.e., Loads 1, 3 and 5) served, we generated 13^3 (2197) scenarios; iii) Topologies 4, 5, and 6 have four loads served, in which 7^4 (2401) scenarios are generated; iv) Under the network Topologies 7 and 8, all five loads are being served in the distribution grid, and as each one is characterized with 5 possible amplitudes for the training process, there are 5^5 (3125), number of scenarios generated. The total number of generated scenarios that contribute to the training dataset is found 19447. All values (e.g., magnitudes and

Table 1: Network Topology Realizations with the Corresponding Number of Generated Scenarios

| Topology | SW1 | SW2 | SW3 | SW4 | SW5 | Number of Scenarios |
|----------|-----|-----|-----|-----|-----|---------------------|
| 1 | 1 | 1 | 0 | 0 | 0 | $1600 (40^2)$ |
| 2 | 1 | 0 | 1 | 0 | 0 | $2197 (13^3)$ |
| 3 | 1 | 0 | 1 | 0 | 1 | $2197 (13^3)$ |
| 4 | 1 | 0 | 1 | 1 | 1 | $2401 (7^4)$ |
| 5 | 1 | 1 | 1 | 0 | 0 | $2401 (7^4)$ |
| 6 | 1 | 1 | 1 | 0 | 1 | $2401 (7^4)$ |
| 7 | 1 | 1 | 1 | 1 | 0 | $3125 (5^5)$ |
| 8 | 1 | 1 | 1 | 1 | 1 | $3125 (5^5)$ |

phase angles of voltage and current) obtained from PMUs are normalized based on the rule of power system calculation [10]. Thus, all numbers in this heatmap (see **Figure 4**) is ranged between 1.05 to -1.05.

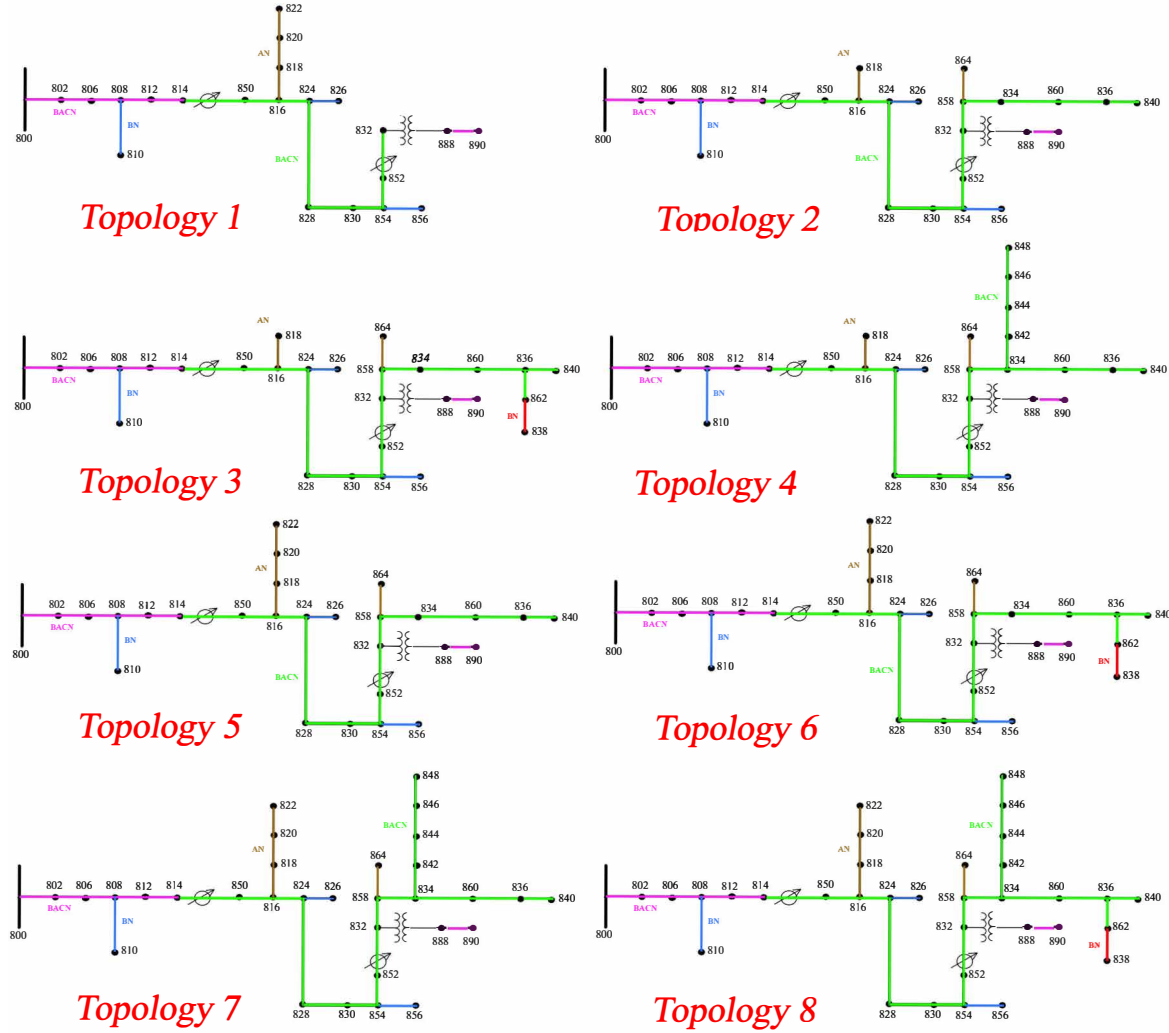


Figure 5: All Studied Network Topologies

2.2 Dataset Preprocessing

In **Figure 4**, the heatmap which generated from Matlab is in "parula" format. However, when we batch-produced heatmaps, we found a problem. The white margin of the image are too wide. If it is used as input, it will cause the input data size to be too large and not compressible and affect the prediction accuracy on the neural network. So we use the pure data form .csv format of the PMU saved by Matlab, and generate heatmaps in batches through python instead, shown in the **Figure 6**.

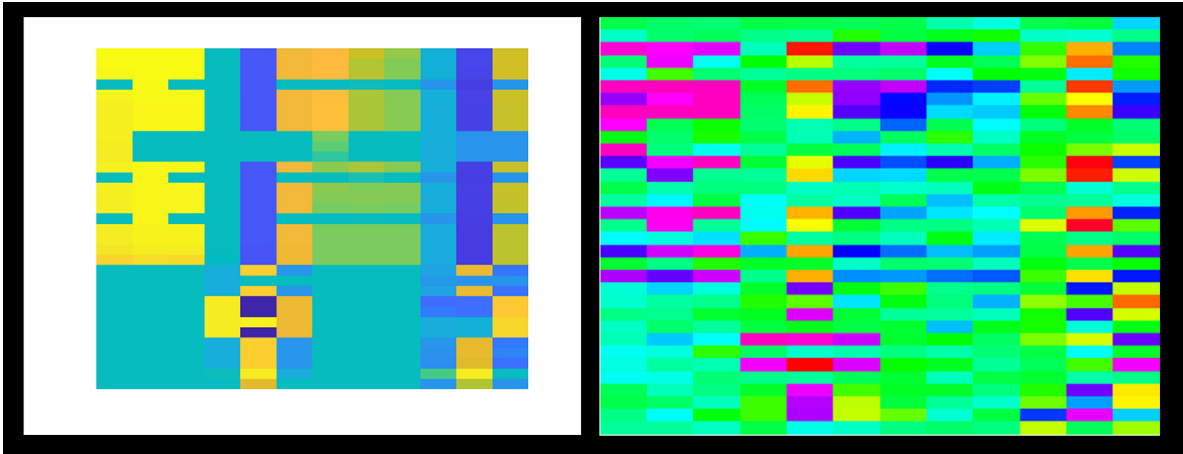


Figure 6: The "parula" heatmap (left) and "gist_rainbow" colormap (right).

So in Python, we used "seaborn.heatmap" library to generate the heatmap [11]. In general format of heatmaps, the single color depth various changes cannot distinguish the data boundary well [12], so we use a colormap format as "gist_rainbow" in generating images as the input of the neural network.

The original size of one heatmap is 497 by 371 pixels, we compressed it into 96 by 96 pixels in the input layer. The RGB heatmap has 3 channels, and we add an additional dimension to save the corresponding label, so the size for the first layer in AE is (96, 96, 4), as the **Figure 1** shown.

3 Model Description

3.1 Ideal Model

For this project, we built an ideal model in addition to two non-ideal models. The ideal model was built in a way that the grid is not affected by any type of noise and that all 33 PMUs are available. However, this ideal model does not reflect real life scenarios, where noise is a big factor affecting the grid and that PMUs are expensive to have at each node. The goal of this ideal model was to show that AE can be implemented and can help in classifying topologies. In this model, we generated ideal images based on the IEEE 34-Node Test Feeder, and built AE in Keras [13].

For building this model, we divided our dataset to 70% for training, 20% for testing, and 10% for validation. Before building the classifier to classify the topologies, we had built an AE that can reconstruct our heatmap images. To use the generated heatmaps, we resized all images to 96×96 and then normalized them by dividing each image by 255. For our AE, we used minibatches because if we used a full batch, the graphical processing unit (GPU) will not be able to handle it. Therefore, for us to pick the right batch size, we picked a large enough value that our model trains better on it yet be supported by the GPU. The batch size we picked was 512. For determining the learning rate, it depends how complex the data is. Since this was an ideal case, a learning rate of 0.01 was good. To check if our learning rate was good, this can be shown in the training loss vs the validation loss plots of the AE. If both losses are decreasing, then our learning rate is performing well with the batch size we had picked. To prevent over fitting in our AE, we defined an early stopping call back with patience equal to 3 and a model check point to save the lowest loss.

As the **Figure 7** shown, the AE we built has 3 layers for encoding, 3 layers for decoding, and one layer for the output. The code for the AE for all models is shown in Appendix B (see **Figure 22**). We used max pooling layer with each dense layer we add. We also used batch normalization and rectified linear activation function (Relu) for each layer except for the output layer, where we used a sigmoid activation function. We used a sigmoid activation function at the output to get an output between 0 and 1

which what each pixel in our image is.

| Layer (type) | Output Shape | Param # |
|-------------------------------|----------------------|---------|
| input_1 (InputLayer) | [None, 96, 96, 4] | 0 |
| conv2d (Conv2D) | (None, 96, 96, 16) | 592 |
| batch_normalization (BatchNo) | (None, 96, 96, 16) | 64 |
| max_pooling2d (MaxPooling2D) | (None, 48, 48, 16) | 0 |
| conv2d_1 (Conv2D) | (None, 48, 48, 32) | 4640 |
| batch_normalization_1 (Batch) | (None, 48, 48, 32) | 128 |
| max_pooling2d_1 (MaxPooling2 | (None, 24, 24, 32) | 0 |
| tf_op_layer_Relu (TensorFlow | [(None, 24, 24, 32)] | 0 |
| conv2d_2 (Conv2D) | (None, 24, 24, 64) | 18496 |
| batch_normalization_2 (Batch) | (None, 24, 24, 64) | 256 |
| max_pooling2d_2 (MaxPooling2 | (None, 12, 12, 64) | 0 |
| conv2d_3 (Conv2D) | (None, 12, 12, 64) | 36928 |
| batch_normalization_3 (Batch) | (None, 12, 12, 64) | 256 |
| up_sampling2d (UpSampling2D) | (None, 24, 24, 64) | 0 |
| conv2d_4 (Conv2D) | (None, 24, 24, 32) | 18464 |
| batch_normalization_4 (Batch) | (None, 24, 24, 32) | 128 |
| up_sampling2d_1 (UpSampling2 | (None, 48, 48, 32) | 0 |
| tf_op_layer_Relu_1 (TensorFl | [(None, 48, 48, 32)] | 0 |
| conv2d_5 (Conv2D) | (None, 48, 48, 16) | 4624 |
| batch_normalization_5 (Batch) | (None, 48, 48, 16) | 64 |
| up_sampling2d_2 (UpSampling2 | (None, 96, 96, 16) | 0 |
| conv2d_6 (Conv2D) | (None, 96, 96, 4) | 580 |
| <hr/> | | |
| Total params: 85,220 | | |
| Trainable params: 84,772 | | |
| Non-trainable params: 448 | | |

Figure 7: The layers information of proposed Autoencoder neural network.

Using the AE we built for the ideal model, we were able to construct a topology classifier [14]. To build that classifier, we got the AE’s encoding layers with their weights

and freeze them. To add fully connected layers for classification purposes, we flattened the last layer in the encoder. After that, we added two fully connected layers with 128 and 8 neurons for the 8 classes, respectively. To tackle over fitting, we added a dropout layer between the two fully connected layers with a value of 0.5. We kept the batch size and the learning rate the same but decrease the epochs from 30 to 10 since the encoding layers are not trainable. To train these classifiers, we used categorical cross-entropy as a loss metric.

3.2 Non-Ideal Models

Since the ideal model does not reflect real-world scenarios, we reconstructed some models that can act like a real-world model. To build these models, we introduced white noise, removed some of the PMUs, and removed random data. We constructed two non-ideal models (10dB SNR white noise and missing one data and 10dB SNR white noise), one with keeping 22 PMUs randomly out of 33 PMUs and adding a 10dB SNR white noise, and the other with also keeping only 22 PMUs, adding 10dB SNR white noise, and randomly removing one data from the matrix. For each non-ideal model, we generated cases based on the IEEE 34-node test feeder taking non-ideality into consideration.

For building these AEs, we divided the generated dataset to 80% for training, 10% for validation, and 10% for testing. To use the generated images, we resized them to 96×96 and normalized them by dividing them by 255. We kept all hyper parameters the same except for the learning rate. For the non-ideal models, we decreased the learning rate to 0.001 because the models now are much complex due to noise and PMU's availability. To tackle over fitting, we also defined an early stopping call back with patience equal to 3 and a model check point to save the lowest loss. Both non-ideal models have the same AE architecture as the ideal model with 3 layers for encoding, 3 layers for decoding, and one layer for the output. We used the same activation functions for all layers as we did for the AE in the ideal model.

Similarly, as we did with the ideal model, we used the AE's encoding layers to help us classify the topologies. So, we set the weights of the encoding layers to the weights

they had at their last epoch and freeze them (not trainable). We then flattened the last encoding layer before adding fully connected layers. Then, we added two fully connected layers with 512 neurons and 8 neurons for the 8 classes, respectively. Similarly, we added a dropout layer of 0.5 between the two fully connected layers. To train these classifiers, we used categorical cross-entropy as a loss metric. All hyper parameters were the same as in the AE model but decreased the epochs from 30 to 10.

4 Numerical Results

4.1 Ideal Models

For all models, we trained the AE at the beginning to make sure that the encoding part is working perfectly so we can use it in the classification model. Here, we start with the results of the ideal model. The training loss v.s. the validation loss plot for the AE for the ideal is shown in **Figure 8**.

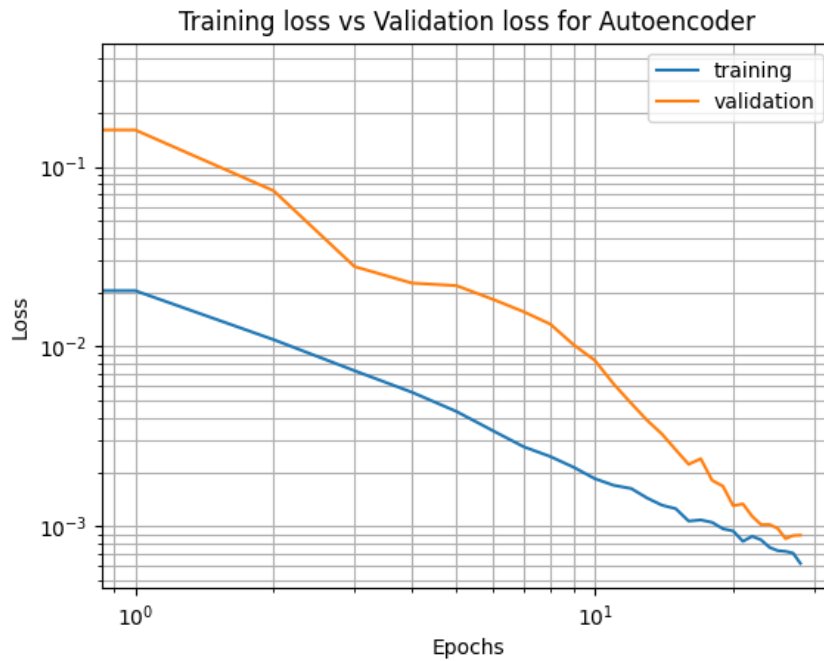


Figure 8: Training loss vs validation loss for AE in the ideal model.

It shows that the model is learning and there is no sign of over fitting since both

losses are decreasing. The AE for the ideal model has been tested on random test set images as shown in **Figure 9**.

Test Images - Encoded Test Images - Reconstructed Test Images

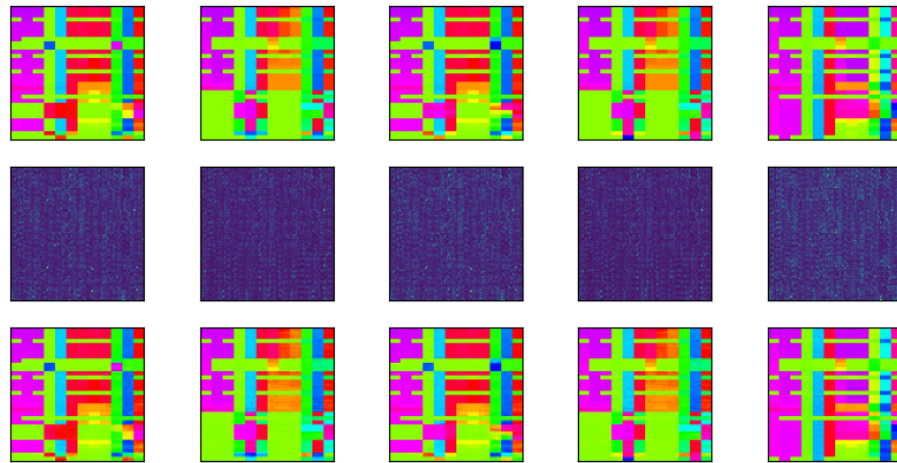


Figure 9: AE prediction on some test set images (Image – Encoding – Decoding).

After we made sure that the classifier is working perfectly, we built the classification model to classify different topologies. The training loss v.s. the validation loss plot for the classifier model is shown in **Figure 10**.



Figure 10: Training loss vs validation loss for the classifier in the ideal model.

Also, the classifier was able to predict all the test set correctly with 100% accuracy as shown in **Figure 11**.

```
Test loss on test set: 4.459287993086036e-06
Test accuracy on test set: 1.0
(3890,) (3890, 8)
Found 3890 correct labels
Found 0 incorrect labels
```

Figure 11: Test accuracy on test set for the ideal model classifier.

This indicates that the classifier was able to predict all unseen images correctly.

4.2 Non-Ideal Models

As we built the ideal model, we built the non-ideal models. We built the AE for each model and made sure that working efficiently. The training loss v.s. validation loss plot for the AE 10dB SNR white noise model is shown in **Figure 12** while the plot for the AE missing one data and 10dB SNR white noise model is shown in **Figure 13**.

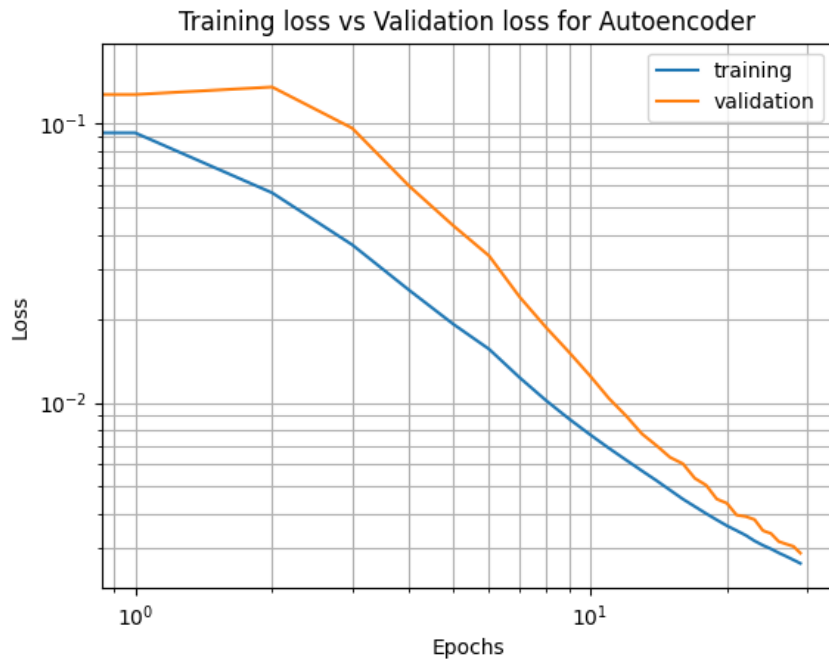


Figure 12: Training loss vs validation loss for the AE 10dB SNR white noise model.

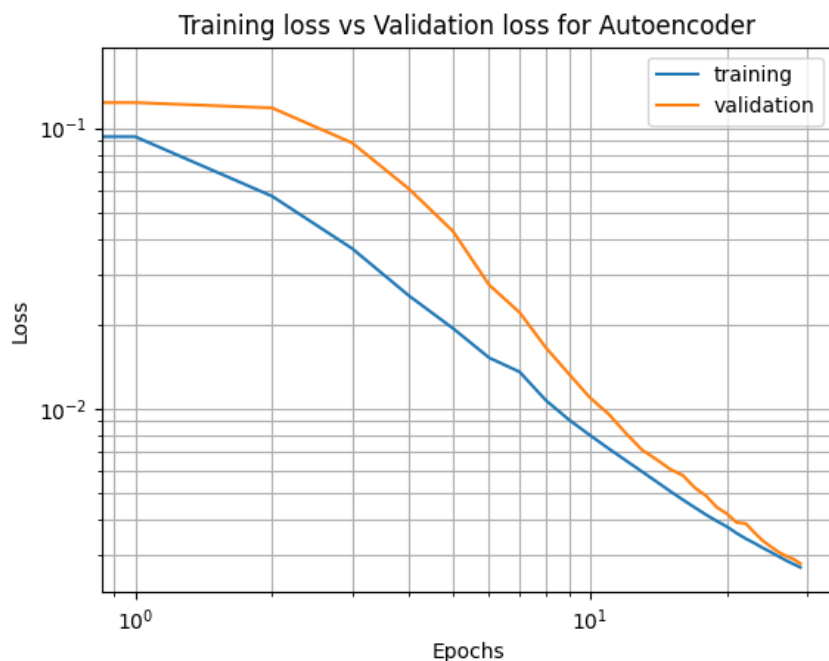


Figure 13: Training loss vs validation loss for the AE missing one data and 10dB SNR white noise model.

These two figures indicate that both AEs were trained efficiently because all losses were decreasing. In addition, since the validation losses are not increasing then the model is not overfitting. Furthermore, **Figure 14** and **Figure 15** show the test of AE of each model on some test images.

Test Images - Encoded Test Images - Reconstructed Test Images

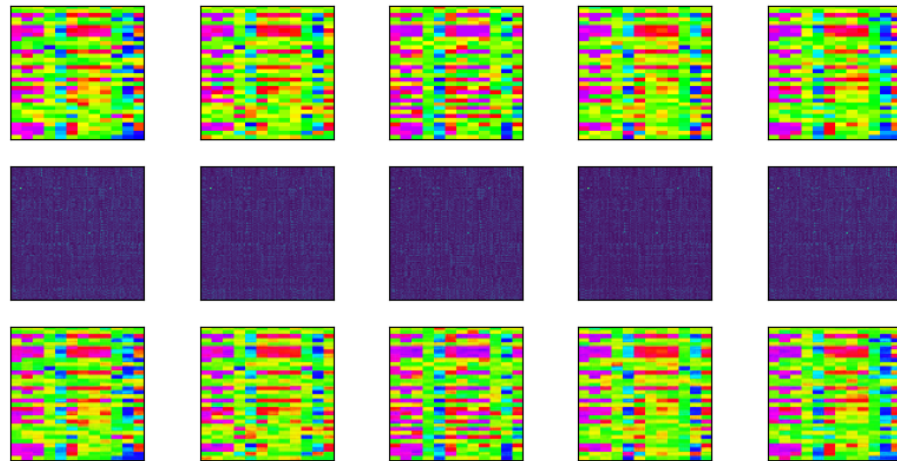


Figure 14: AE 10dB SNR white noise model prediction on some test set images (Image – Encoding – Decoding).

Test Images - Encoded Test Images - Reconstructed Test Images

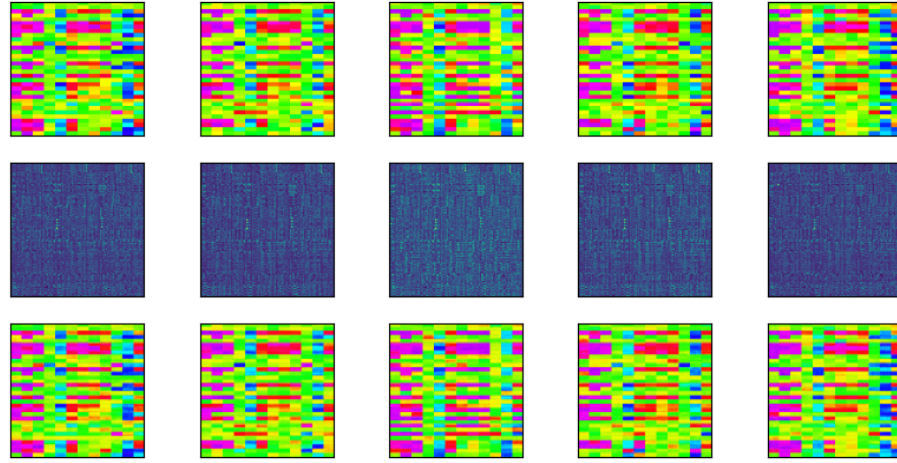


Figure 15: AE missing one data and 10dB SNR white nosie model prediction on some test set images (Image – Encoding – Decoding).

Since the AEs for each non-ideal model is working efficiently and perfectly, we built the classifier using the encoding layers and some fully connected layers. The training loss vs the validation loss plots for each classifier is shown in **Figure 16** and **Figure 17**.

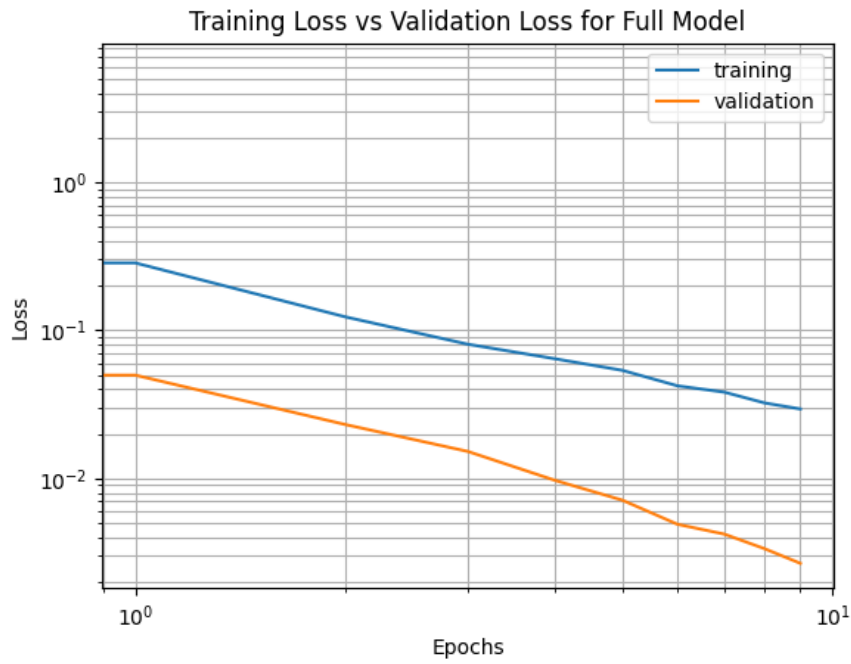


Figure 16: Training loss vs validation loss for the 10dB SNR white noise model classifier.

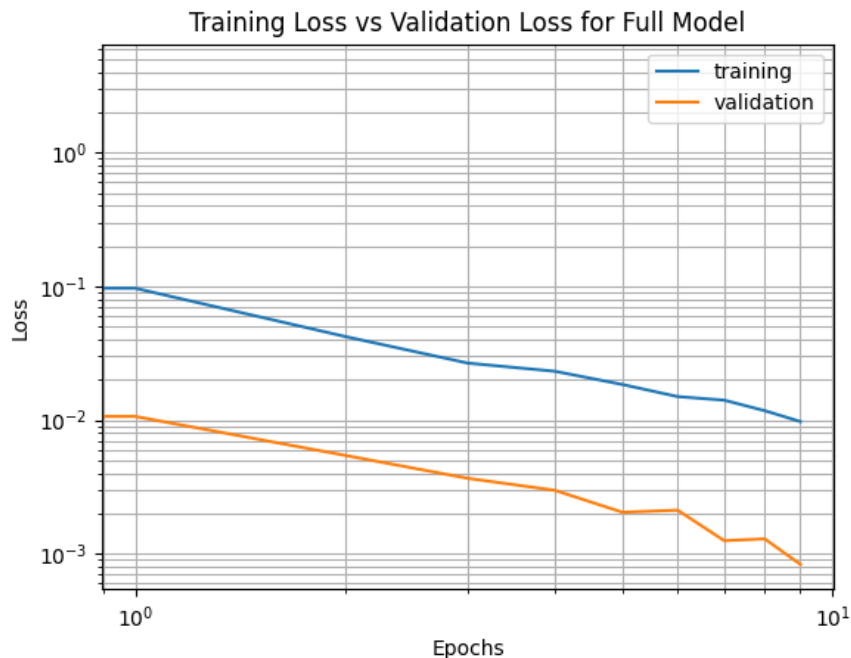


Figure 17: Training loss vs validation loss for the missing one data and 10dB SNR white noise model classifier.

The classifiers were able to predict all test set images correctly with 100% accuracy as shown in **Figure 18** and **Figure 19**.

```
Test loss on test set: 0.002677673939615488
Test accuracy on test set: 1.0
(1944,) (1944, 8)
Found 1944 correct labels
Found 0 incorrect labels
```

Figure 18: Test accuracy on test set for the 10dB SNR white noise model classifier.

```
Test loss on test set: 0.0008325269445776939
Test accuracy on test set: 1.0
(1944,) (1944, 8)
Found 1944 correct labels
Found 0 incorrect labels
```

Figure 19: Test accuracy on test set for the missing one data and 10dB SNR white noise model classifier.

This indicates the model has been trained efficiently and that there is no sign of over fitting in these models.

4.3 Models Test on Interfered Datasets

The dataset we used to build the ideal and non-ideal models had a load change from 95% to 105%, and these models were tested on 3 new interfered datasets that had a load change from 93% to 95% and 105% to 107%. Furthermore, two of these interfered datasets have missing value/s from their matrices. These interfered datasets were not seen by any of the models (new to the trained models) trained in section 4.1 and section 4.2, thus it is expected to get low accuracy. Since the trained models were not reproducible, even though we have set the seed for cuDNN, random, and TensorFlow, we generated 5 to 10 batches for each model we had. We then took all these batch results and predicted each interfered dataset and average all results to get a value for each model. These results are shown in **Table 2**. The first column in **Table 2** stands for the models we built in section 4.1 and section 4.2 while the first row stands

for the 3 interfered datasets we introduced above. Looking at **Table 2**, no matter which model we pick, the prediction accuracy decreases as we move from left to right because the interfered dataset gets "worse"; It fits the common sense of deep learning. The accuracies of the non-ideal models are acceptable unlike the accuracies of the ideal model. This could be due to that non-ideal models took white noise and missing data in building the model into considerations while ideal model did not. Finally, although the shape of the topology is different, we realized that for "Topology 2" and "Topology 3" switching the breaker SW 5 does not influence the PMU data too much because there is no load on circuit branch node 862 - node 838. Hence, the data of "Topology 2" and "Topology 3" are almost the same.

Table 2: The prediction accuracy (%) by training and testing the AE in different extents of interferences for 8 topologies

| Models | Interfered Data | 40dB SNR | Missing One Data | Missing Two Data |
|---|-----------------|----------|-------------------|-------------------|
| | | | based on 40dB SNR | based on 40dB SNR |
| Ideal Model (33 PMU with no Missing and 0dB SNR) | | 55.357 | 55.214 | 55.125 |
| 22 PMU with no Missing and 10dB SNR Model | | 86.571 | 86.482 | 86.053 |
| 22 PMU with Missing One Data and 10dB SNR Model | | 77.373 | 76.998 | 76.374 |

4.4 For 7 Topologies

As we known the reason for low accuracy, we removed "Topology 3" from the system, in another word, we removed "label 3" in the input and output layers. And now, there are 7 topologies in total, and we tested them again, shown below:

Table 3: The prediction accuracy (%) by training and testing the AE in different extents of interferences for 7 topologies

| Models \ Interfered Data | 40dB SNR | Missing One Data based on 40dB SNR | Missing Two Data based on 40dB SNR |
|---|----------|------------------------------------|------------------------------------|
| Ideal Model (33 PMU with no Missing and 0dB SNR) | 79.571 | 79.381 | 79.285 |
| 22 PMU with no Missing and 10dB SNR Model | 71.476 | 71.428 | 71.428 |

The prediction accuracy increased dramatically to nearly 80% from 55%. And it means our assumption is right, "Topology 3" indeed badly influenced the accuracy. But within the same structure on the non-ideal model "22 PMU with 10dB SNR", the accuracy went down, that is because once the input changed, the neural network also need to adjust to fit that change. However, due to time constraints, this project will stop here. How to improve the neural network structure to adapt to the new input will left to the future research.

5 Conclusion

In this project, a deep learning AE framework is proposed for online detection of power distribution system topology. The proposed AE framework can handle missing measurements under unbalanced operating states. The experiments show that the proposed AE not only handles the data with the same level of interference (noise and missing measurements), but also has the capacity of estimating the interfered data which has different distributions from the training examples. Numerical experiments proved

that our trained network can accurately identify the network topology corresponding to the observed data beyond the training dataset.

Future work could be targeted at implementing the proposed framework on a larger real-world power grid, such as the IEEE 123-bus test system, and validating the results' accuracy and computational effectiveness during real-time applications. Moreover, the architecture of the proposed AE neural network could be optimized for increasing the prediction accuracy of general models for improving universality.

References

- [1] National Academies of Sciences, *Enhancing the resilience of the nation's electricity system*. National Academies Press, 2017.
- [2] National Centers for Environmental Information, “Billion-dollar weather and climate disasters: Overview,” 2020. [Online] Available at: <https://www.ncdc.noaa.gov/billions/>.
- [3] Wikipedia, “Phasor measure unit,” 2020. [Online] Available at: https://en.wikipedia.org/wiki/Phasor_measurement_unit.
- [4] C. M. Davis, J. E. Tate, and T. J. Overbye, “Wide area phasor data visualization,” in *2007 39th North American Power Symposium*, pp. 246–252, 2007.
- [5] E. Lawrence, S. V. Wiel, and R. Bent, “Model bank state estimation for power grids using importance sampling,” *Technometrics*, vol. 55, no. 4, pp. 426–435, 2013.
- [6] G. Cavraro and R. Arghandeh, “Power distribution network topology detection with time-series signature verification method,” *IEEE Transactions on Power Systems*, vol. 33, no. 4, pp. 3500–3509, 2018.
- [7] D. Deka, S. Talukdar, M. Chertkov, and M. V. Salapaka, “Graphical models in meshed distribution grids: Topology estimation, change detection & limitations,” *IEEE Transactions on Smart Grid*, vol. 11, no. 5, pp. 4299–4310, 2020.
- [8] “Autoencoder.” [Online] Available at: <https://en.wikipedia.org/wiki/Autoencoder>, Accessed:2020.
- [9] IEEE PES, “34-bus feeder case,” 2010. [Online] Available at: <https://site.ieee.org/pes-testfeeders/resources>.
- [10] J. D. Glover, M. S. Sarma, and T. Overbye, *Power system analysis & design, SI version*. Cengage Learning, 2012.
- [11] “seaborn.heatmap.” [Online] Available at: <https://seaborn.pydata.org/generated/seaborn.heatmap.html>, Accessed:2020.

- [12] “How bad is your colormap?.” [Online] Available at: <http://jakevdp.github.io/blog/2014/10/16/how-bad-is-your-colormap/>, Accessed:2020.
- [13] A. Sharma, “Implementing autoencoders in keras: Tutorial.” [Online] Available at: <https://www.datacamp.com/community/tutorials/autoencoder-keras-tutorial#cae>, Accessed:2020.
- [14] A. Sharma, “Autoencoder as a classifier using fashion-mnist dataset.” [Online] Available at: <https://www.datacamp.com/community/tutorials/autoencoder-classifier-python#>, Accessed:2020.
- [15] Y. Li, *Date-Driven Topology Identification in Power Distribution Systems with Machine Learning*. PhD thesis, The George Washington University, 2020.

Appendix A: IEEE 34 Node Test Feeder

Introduction

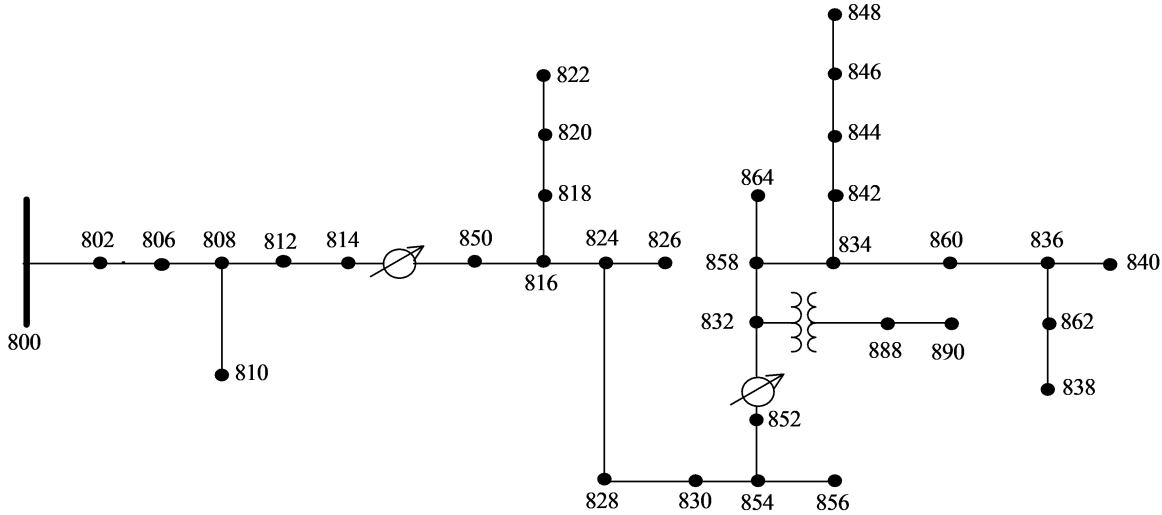


Figure 20: IEEE 34-Node Test Feeder [9]

This feeder is an actual feeder located in Arizona. The feeder's nominal voltage is 24.9 kV. It is characterized by:

- (1) Very long and lightly loaded overhead distribution lines
- (2) Two in-line regulators required to maintain a good voltage profile across the network
- (3) A wye-wye grounded transformer reducing the voltage to 4.16 kV for a short section of the feeder
- (4) 24 unbalanced loading with both "spot" and "distributed" loads. Distributed loads are assumed to be evenly distributed on the distribution line.
- (5) Shunt capacitors

System Data

Here are the data forms originated from the IEEE PES AMPS DSAS test feeder working group [9].

Table 4: Overhead Line Configurations [9]

| Config. | Phasing | Phase ACSR ¹ | Neutral ACSR | Spacing ID |
|---------|---------|-------------------------|--------------|------------|
| 300 | BACN | 1/0 | 1/0 | 500 |
| 301 | BACN | #2 6/1 | #2 6/1 | 500 |
| 302 | AN | #4 6/1 | #4 6/1 | 510 |
| 303 | BN | #4 6/1 | #4 6/1 | 510 |
| 304 | BN | #2 6/1 | #2 6/1 | 510 |

¹ ACSR: Aluminum conductor steel reinforced.

Table 5: Line Segment Data [9]

| Node A | Node B | Length (ft.) | Config. |
|--------|--------|--------------|---------|
| 800 | 802 | 2580 | 300 |
| 802 | 806 | 1730 | 300 |
| 806 | 808 | 32230 | 300 |
| 808 | 810 | 5804 | 303 |
| 808 | 812 | 37500 | 300 |
| 812 | 814 | 29730 | 300 |
| 814 | 850 | 10 | 301 |
| 816 | 818 | 1710 | 302 |
| 816 | 824 | 10210 | 301 |
| 818 | 820 | 48150 | 302 |
| 820 | 822 | 13740 | 302 |
| 824 | 826 | 3030 | 303 |
| 824 | 828 | 840 | 301 |

| | | | |
|-----|-----|-------|-------|
| 828 | 830 | 20440 | 301 |
| 830 | 854 | 520 | 301 |
| 832 | 858 | 4900 | 301 |
| 832 | 888 | 0 | XFM-1 |
| 834 | 860 | 2020 | 301 |
| 834 | 842 | 280 | 301 |
| 836 | 840 | 860 | 301 |
| 836 | 862 | 280 | 301 |
| 842 | 844 | 1350 | 301 |
| 844 | 846 | 3640 | 301 |
| 846 | 848 | 530 | 301 |
| 850 | 816 | 130 | 301 |
| 852 | 832 | 10 | 301 |
| 854 | 856 | 23330 | 303 |
| 854 | 852 | 36830 | 301 |
| 858 | 864 | 1620 | 302 |
| 858 | 834 | 5830 | 301 |
| 860 | 836 | 2680 | 301 |
| 862 | 838 | 4860 | 304 |
| 888 | 890 | 10560 | 300 |

Table 6: Transformer Data [9]

| | kVA | kV - high | kV - low | R - % | X - % |
|-------------------|------|-------------|-------------|-------|-------|
| Substation | 2500 | 69 - D | 24.9 - Gr.W | 1 | 8 |
| XFM-1 | 500 | 24.9 - Gr.W | 24.9 - Gr.W | 1.9 | 4.08 |

Table 7: Spot Loads [9]

| Node | Load | Ph-1 | Ph-1 | Ph-2 | Ph-2 | Ph-3 | Ph-4 |
|-------|-------|------|------|------|------|------|------|
| | Model | kW | kVAr | kW | kVAr | kW | kVAr |
| 860 | Y-PQ | 20 | 16 | 20 | 16 | 20 | 16 |
| 802 | Y-I | 9 | 7 | 9 | 7 | 9 | 7 |
| 806 | Y-Z | 135 | 105 | 135 | 105 | 135 | 105 |
| 808 | D-PQ | 20 | 16 | 20 | 16 | 20 | 16 |
| 808 | D-I | 150 | 75 | 150 | 75 | 150 | 75 |
| 812 | D-Z | 10 | 5 | 10 | 5 | 25 | 10 |
| Total | | 344 | 224 | 344 | 224 | 359 | 229 |

Impedances

Configuration 300:

———— Z & B Matrices Before Changes ————

Z (R +jX) in ohms per mile

| | | | | | |
|--------|--------|--------|--------|--------|--------|
| 1.3368 | 1.3343 | 0.2101 | 0.5779 | 0.2130 | 0.5015 |
| | | 1.3238 | 1.3569 | 0.2066 | 0.4591 |
| | | | | 1.3294 | 1.3471 |

B in micro Siemens per mile

| | | |
|--------|---------|---------|
| 5.3350 | -1.5313 | -0.9943 |
| 5.0979 | -0.6212 | |
| | 4.8880 | |

Configuration 301:

Z (R +jX) in ohms per mile

| | | | | | |
|--------|--------|--------|--------|--------|--------|
| 1.9300 | 1.4115 | 0.2327 | 0.6442 | 0.2359 | 0.5691 |
| | | 1.9157 | 1.4281 | 0.2288 | 0.5238 |
| | | | | 1.9219 | 1.4209 |

B in micro Siemens per mile

| | | |
|--------|---------|---------|
| 5.1207 | -1.4364 | -0.9402 |
| 4.9055 | -0.5951 | |
| | 4.7154 | |

Configuration 302:

Table 8: Distributed Loads [9]

| Node | Node | Load | Ph-1 | Ph-1 | Ph-2 | Ph-2 | Ph-3 | Ph-3 |
|-------|------|-------|------|------|------|------|------|------|
| A | B | Model | kW | kVAr | kW | kVAr | kW | kVAr |
| 802 | 806 | Y-PQ | 0 | 0 | 30 | 15 | 25 | 14 |
| 808 | 810 | Y-I | 0 | 0 | 16 | 8 | 0 | 0 |
| 818 | 820 | Y-Z | 34 | 17 | 0 | 0 | 0 | 0 |
| 820 | 822 | Y-PQ | 135 | 70 | 0 | 0 | 0 | 0 |
| 816 | 824 | D-I | 0 | 0 | 5 | 2 | 0 | 0 |
| 824 | 826 | Y-I | 0 | 0 | 40 | 20 | 0 | 0 |
| 824 | 828 | Y-PQ | 0 | 0 | 0 | 0 | 4 | 2 |
| 828 | 830 | Y-PQ | 7 | 3 | 0 | 0 | 0 | 0 |
| 854 | 856 | Y-PQ | 0 | 0 | 4 | 2 | 0 | 0 |
| 832 | 858 | D-Z | 7 | 3 | 2 | 1 | 6 | 3 |
| 858 | 864 | Y-PQ | 2 | 1 | 0 | 0 | 0 | 0 |
| 858 | 834 | D-PQ | 4 | 2 | 15 | 8 | 13 | 7 |
| 834 | 860 | D-Z | 16 | 8 | 20 | 10 | 110 | 55 |
| 860 | 836 | D-PQ | 30 | 15 | 10 | 6 | 42 | 22 |
| 836 | 840 | D-I | 18 | 9 | 22 | 11 | 0 | 0 |
| 862 | 838 | Y-PQ | 0 | 0 | 28 | 14 | 0 | 0 |
| 842 | 844 | Y-PQ | 9 | 5 | 0 | 0 | 0 | 0 |
| 844 | 846 | Y-PQ | 0 | 0 | 25 | 12 | 20 | 11 |
| 846 | 848 | Y-PQ | 0 | 0 | 23 | 11 | 0 | 0 |
| Total | | | 262 | 133 | 240 | 120 | 220 | 114 |

Table 9: Shunt Capacitors [9]

| Node | Ph-A | Ph-B | Ph-C |
|-------|------|------|------|
| | kVAr | kVAr | kVAr |
| 844 | 100 | 100 | 100 |
| 848 | 150 | 150 | 150 |
| Total | 250 | 250 | 250 |

Table 10: Regulator Data [9]

| | | | | | | |
|-----------------------------|-----------|------|------|-----------|------|------|
| Regulator ID | 1 | | | 2 | | |
| Line Segment | 814-850 | | | 852-832 | | |
| Location | 814 | | | 852 | | |
| Phases | A-B-C | | | A-B-C | | |
| Connection | 3-Ph, LG | | | 3-Ph, LG | | |
| Monitoring Phase | A-B-C | | | A-B-C | | |
| Bandwidth | 2.0 volts | | | 2.0 volts | | |
| PT Ratio | 120 | | | 120 | | |
| Primary CT Rating | 100 | | | 100 | | |
| Compensator Settings | Ph-A | Ph-B | Ph-C | Ph-A | Ph-B | Ph-C |
| R-Setting | 2.7 | 2.7 | 2.7 | 2.5 | 2.5 | 2.5 |
| X-Setting | 1.6 | 1.6 | 1.6 | 1.6 | 1.6 | 1.6 |
| Vlotage Level | 122 | 122 | 122 | 124 | 124 | 124 |

| | | | | | |
|-----------------------------|--------|--------|--------|--------|--------|
| Z (R +jX) in ohms per mile | | | | | |
| 2.7995 | 1.4855 | 0.0000 | 0.0000 | 0.0000 | 0.0000 |
| | | 0.0000 | 0.0000 | 0.0000 | 0.0000 |
| | | | 0.0000 | 0.0000 | |
| B in micro Siemens per mile | | | | | |
| | 4.2251 | 0.0000 | 0.0000 | | |
| | | 0.0000 | 0.0000 | | |
| | | | 0.0000 | | |

Configuration 303:

| | | | | | |
|-----------------------------|--------|--------|--------|--------|--------|
| Z (R +jX) in ohms per mile | | | | | |
| 0.0000 | 0.0000 | 0.0000 | 0.0000 | 0.0000 | 0.0000 |
| | 2.7995 | 1.4855 | 0.0000 | 0.0000 | |
| | | | 0.0000 | 0.0000 | |
| B in micro Siemens per mile | | | | | |
| | 0.0000 | 0.0000 | 0.0000 | | |
| | 4.2251 | 0.0000 | | | |
| | | 0.0000 | | | |

Configuration 304:

| | | | | | |
|-----------------------------|--------|--------|--------|--------|--------|
| Z (R +jX) in ohms per mile | | | | | |
| 0.0000 | 0.0000 | 0.0000 | 0.0000 | 0.0000 | 0.0000 |
| | 1.9217 | 1.4212 | 0.0000 | 0.0000 | |
| | | | 0.0000 | 0.0000 | |
| B in micro Siemens per mile | | | | | |
| | 0.0000 | 0.0000 | 0.0000 | | |
| | 4.3637 | 0.0000 | | | |
| | | 0.0000 | | | |

Power Flow Results

Radial Flow Summary

— R A D I A L F L O W S U M M A R Y — DATE: 6-24-2004 AT 16:34:11 HOURS —
 SUBSTATION: IEEE 34; FEEDER: IEEE 34

| SYSTEM | PHASE (A) | PHASE (B) | PHASE (C) | TOTAL |
|----------------|--------------|--------------|--------------|--------------------|
| INPUT | | | | |
| kW : 759.136 | | 666.663 | | 617.072 2042.872 |
| kVAr : 171.727 | | 90.137 | | 28.394 290.258 |
| kVA : 778.318 | | 672.729 | | 617.725 2063.389 |

| | | | | | | | | | | | |
|--|---------|-------|---------|-------|---------|--|----------|-------|--|--------|-------|
| PF | .9754 | | .9910 | | .9989 | | .9901 | | | | |
| LOAD —(A-N)——(A-B)--- (B-N)——(B-C)--- (C-N)——(C-A)--- WYE——DELTA— | | | | | | | | | | | |
| kW | 359.9 | 246.4 | | 339.3 | 243.3 | | 221.8 | 359.0 | | 921.0 | 848.8 |
| TOT | 606.322 | | 582.662 | | 580.840 | | 1769.824 | | | | |
| | | | | | | | | | | | |
| kVAr | 230.9 | 128.7 | | 216.9 | 128.7 | | 161.8 | 184.6 | | 609.6 | 441.9 |
| TOT | 359.531 | | 345.609 | | 346.407 | | 1051.547 | | | | |
| | | | | | | | | | | | |
| kVA | 427.6 | 278.0 | | 402.7 | 275.3 | | 274.6 | 403.7 | | 1104.5 | 957.0 |
| TOT | 704.903 | | 677.452 | | 676.293 | | 2058.647 | | | | |
| | | | | | | | | | | | |
| PF | .8417 | .8864 | | .8425 | .8840 | | .8078 | .8894 | | .8339 | .8870 |
| TOT | .8601 | | .8601 | | .8589 | | .8597 | | | | |
| LOSSES —(A)—— (B)—— (C)—— | | | | | | | | | | | |
| kW | 114.836 | | 80.389 | | 77.824 | | 273.049 | | | | |
| kVAr | 14.200 | | 10.989 | | 9.810 | | 34.999 | | | | |
| kVA | 115.711 | | 81.137 | | 78.440 | | 275.283 | | | | |
| CAPAC —(A-N)——(A-B)--- (B-N)——(B-C)--- (C-N)——(C-A)--- WYE——DELTA— | | | | | | | | | | | |
| R-kVA: | 250.0 | .0 | | 250.0 | .0 | | 250.0 | .0 | | 750.0 | .0 |
| TOT | 250.000 | | 250.000 | | 250.000 | | 750.000 | | | | |
| | | | | | | | | | | | |
| A-kVA: | 265.7 | .0 | | 264.8 | .0 | | 265.9 | .0 | | 796.3 | .0 |
| TOT | 265.658 | | 264.760 | | 265.869 | | 796.287 | | | | |

Voltage Profile

— V O L T A G E P R O F I L E —— DATE: 6-24-2004 AT 16:34:18 HOURS ——
SUBSTATION: IEEE 34; FEEDER: IEEE 34

| NODE | MAG | ANGLE | MAG | ANGLE | MAG | ANGLE | mi. to SR |
|------|-----------------|-------|-------------------|-------|------------------|-------|-----------|
| | A-N | | B-N | | C-N | | |
| 800 | 1.0500 at .00 | | 1.0500 at -120.00 | | 1.0500 at 120.00 | | .000 |
| 802 | 1.0475 at -.05 | | 1.0484 at -120.07 | | 1.0484 at 119.95 | | .489 |
| 806 | 1.0457 at -.08 | | 1.0474 at -120.11 | | 1.0474 at 119.92 | | .816 |
| 808 | 1.0136 at -.75 | | 1.0296 at -120.95 | | 1.0289 at 119.30 | | 6.920 |
| 810 | | | 1.0294 at -120.95 | | | | 8.020 |
| 812 | .9763 at -1.57 | | 1.0100 at -121.92 | | 1.0069 at 118.59 | | 14.023 |
| 814 | .9467 at -2.26 | | .9945 at -122.70 | | .9893 at 118.01 | | 19.653 |
| RG10 | 1.0177 at -2.26 | | 1.0255 at -122.70 | | 1.0203 at 118.01 | | 19.654 |
| 850 | 1.0176 at -2.26 | | 1.0255 at -122.70 | | 1.0203 at 118.01 | | 19.655 |
| 816 | 1.0172 at -2.26 | | 1.0253 at -122.71 | | 1.0200 at 118.01 | | 19.714 |

| | | | | | | | | | | | | | | |
|------|--|--------|----|-------|--|--------|----|---------|--|--------|--------|--------|--|--------|
| 818 | | 1.0163 | at | -2.27 | | | | | | | 20.038 | | | |
| 820 | | .9926 | at | -2.32 | | | | | | | 29.157 | | | |
| 822 | | .9895 | at | -2.33 | | | | | | | 31.760 | | | |
| 824 | | 1.0082 | at | -2.37 | | 1.0158 | at | -122.94 | | 1.0116 | at | 117.76 | | 21.648 |
| 826 | | | | | | 1.0156 | at | -122.94 | | | | 22.222 | | |
| 828 | | 1.0074 | at | -2.38 | | 1.0151 | at | -122.95 | | 1.0109 | at | 117.75 | | 21.807 |
| 830 | | .9894 | at | -2.63 | | .9982 | at | -123.39 | | .9938 | at | 117.25 | | 25.678 |
| 854 | | .9890 | at | -2.64 | | .9978 | at | -123.40 | | .9934 | at | 117.24 | | 25.777 |
| 852 | | .9581 | at | -3.11 | | .9680 | at | -124.18 | | .9637 | at | 116.33 | | 32.752 |
| RG11 | | 1.0359 | at | -3.11 | | 1.0345 | at | -124.18 | | 1.0360 | at | 116.33 | | 32.752 |
| 832 | | 1.0359 | at | -3.11 | | 1.0345 | at | -124.18 | | 1.0360 | at | 116.33 | | 32.754 |
| 858 | | 1.0336 | at | -3.17 | | 1.0322 | at | -124.28 | | 1.0338 | at | 116.22 | | 33.682 |
| 834 | | 1.0309 | at | -3.24 | | 1.0295 | at | -124.39 | | 1.0313 | at | 116.09 | | 34.786 |
| 842 | | 1.0309 | at | -3.25 | | 1.0294 | at | -124.39 | | 1.0313 | at | 116.09 | | 34.839 |
| 844 | | 1.0307 | at | -3.27 | | 1.0291 | at | -124.42 | | 1.0311 | at | 116.06 | | 35.095 |
| 846 | | 1.0309 | at | -3.32 | | 1.0291 | at | -124.46 | | 1.0313 | at | 116.01 | | 35.784 |
| 848 | | 1.0310 | at | -3.32 | | 1.0291 | at | -124.47 | | 1.0314 | at | 116.00 | | 35.885 |
| 860 | | 1.0305 | at | -3.24 | | 1.0291 | at | -124.39 | | 1.0310 | at | 116.09 | | 35.169 |
| 836 | | 1.0303 | at | -3.23 | | 1.0287 | at | -124.39 | | 1.0308 | at | 116.09 | | 35.677 |
| 840 | | 1.0303 | at | -3.23 | | 1.0287 | at | -124.39 | | 1.0308 | at | 116.09 | | 35.839 |
| 862 | | 1.0303 | at | -3.23 | | 1.0287 | at | -124.39 | | 1.0308 | at | 116.09 | | 35.730 |
| 838 | | | | | | 1.0285 | at | -124.39 | | | | 36.650 | | |
| 864 | | 1.0336 | at | -3.17 | | | | | | | | 33.989 | | |
| XF10 | | .9997 | at | -4.63 | | .9983 | at | -125.73 | | 1.0000 | at | 114.82 | | 32.754 |
| 888 | | .9996 | at | -4.64 | | .9983 | at | -125.73 | | 1.0000 | at | 114.82 | | 32.754 |
| 890 | | .9167 | at | -5.19 | | .9235 | at | -126.78 | | .9177 | at | 113.98 | | 34.754 |
| 856 | | | | | | .9977 | at | -123.41 | | | | 30.195 | | |

Voltage Regulator Data

| VOLTAGE REGULATOR DATA | | | | | | | | DATE: | 6-24-2004 AT 16:34:22 HOURS | |
|--------------------------------------|----------|------------|-------------|----------------------|----------|---------|-----|-------|-----------------------------|--|
| SUBSTATION: IEEE 34; FEEDER: IEEE 34 | | | | | | | | | | |
| <hr/> | | | | | | | | | | |
| [NODE] | --[VREG] | -----[SEG] | -----[NODE] | MODEL | | | | OPT | BNDW | |
| 814 | RG10 | 850 | 850 | Phase A & B & C, Wye | | | | RX | 2.00 | |
| <hr/> | | | | | | | | | | |
| PHASE | LDCTR | VOLT HOLD | R-VOLT | X-VOLT | PT RATIO | CT RATE | TAP | | | |
| 1 | | 122.000 | 2.700 | 1.600 | 120.00 | 100.00 | 12 | | | |
| 2 | | 122.000 | 2.700 | 1.600 | 120.00 | 100.00 | 5 | | | |
| 3 | | 122.000 | 2.700 | 1.600 | 120.00 | 100.00 | 5 | | | |
| <hr/> | | | | | | | | | | |
| [NODE] | --[VREG] | -----[SEG] | -----[NODE] | MODEL | | | | OPT | BNDW | |
| 852 | RG11 | 832 | 832 | Phase A & B & C, Wye | | | | RX | 2.00 | |
| <hr/> | | | | | | | | | | |
| PHASE | LDCTR | VOLT HOLD | R-VOLT | X-VOLT | PT RATIO | CT RATE | TAP | | | |

| | | | | | | |
|---|---------|-------|-------|--------|--------|----|
| 1 | 124.000 | 2.500 | 1.500 | 120.00 | 100.00 | 13 |
| 2 | 124.000 | 2.500 | 1.500 | 120.00 | 100.00 | 11 |
| 3 | 124.000 | 2.500 | 1.500 | 120.00 | 100.00 | 12 |

Radial Power Flow

| — R A D I A L P O W E R F L O W — DATE: 6-24-2004 AT 16:34:32 HOURS — | | | | | |
|---|----------------|---|---------------------|---------------------|------------------|
| SUBSTATION: IEEE 34; FEEDER: IEEE 34 | | | | | |
| NODE | VALUE | PHASE A (LINE A) | PHASE B (LINE B) | PHASE C (LINE C) | UNT O/L< 60.% |
| * | * | A | B | C | * |
| NODE: 800 | VOLTS: | 1.050 .00 | 1.050 -120.00 | 1.050 120.00 | MAG/ANG |
| kVll | 24.900 | NO LOAD OR CAPACITOR REPRESENTED AT SOURCE NODE | | | |
| TO NODE 802 | : 51.56 -12.74 | 44.57 -127.70 | 40.92 117.37 | AMP/DG | |
| <802 > LOSS= 3.472: | : (1.637) | (.978) | (.858) | kW | |
| * | * | A | B | C | * |
| NODE: 802 | VOLTS: | 1.047 -.05 | 1.048 -120.07 | 1.048 119.95 | MAG/ANG |
| | -LD: | .00 .00 | .00 .00 | .00 .00 | kW/kVR |
| kVll | 24.900 | CAP: | .00 | .00 | .00 kVR |
| FROM NODE 800 | : 51.58 -12.80 | 44.57 -127.76 | 40.93 117.31 | AMP/DG | |
| <802 > LOSS= 3.472: | : (1.637) | (.978) | (.858) | kW | |
| TO NODE 806 | : 51.58 -12.80 | 44.57 -127.76 | 40.93 117.31 | AMP/DG | |
| <806 > LOSS= 2.272: | : (1.102) | (.618) | (.552) | kW | |
| * | * | A | B | C | * |
| NODE: 806 | VOLTS: | 1.046 -.08 | 1.047 -120.11 | 1.047 119.92 | MAG/ANG |
| | -LD: | .00 .00 | .00 .00 | .00 .00 | kW/kVR |
| kVll | 24.900 | CAP: | .00 | .00 | .00 kVR |
| FROM NODE 802 | : 51.59 -12.83 | 42.47 -126.83 | 39.24 118.52 | AMP/DG | |
| <806 > LOSS= 2.272: | : (1.102) | (.618) | (.552) | kW | |
| TO NODE 808 | : 51.59 -12.83 | 42.47 -126.83 | 39.24 118.52 | AMP/DG | |
| <808 > LOSS= 41.339: | : (20.677) | (10.780) | (9.882) | kW | |
| * | * | A | B | C | * |
| NODE: 808 | VOLTS: | 1.014 -.75 | 1.030 -120.95 | 1.029 119.30 | MAG/ANG |
| | -LD: | .00 .00 | .00 .00 | .00 .00 | kW/kVR |
| kVll | 24.900 | CAP: | .00 | .00 | .00 kVR |
| FROM NODE 806 | : 51.76 -13.47 | 42.46 -127.59 | 39.28 117.76 | AMP/DG | |
| <808 > LOSS= 41.339: | : (20.677) | (10.780) | (9.882) | kW | |
| TO NODE 810 | | 1.22 -144.62 | | AMP/DG | |
| <810 > LOSS= .002: | | (.002) | | kW | |
| TO NODE 812 | : 51.76 -13.47 | 41.30 -127.10 | 39.28 117.76 | AMP/DG | |

| | | | | | | |
|----------------------|--------------|---------------|---------------------|---------------------|-----------|----------------------|
| <812 | > LOSS= | 47.531: | (24.126) | (11.644) | (11.761) | kW |
| | * | A | * | B | * | C |
| NODE: 810 | VOLTS: | | 1.029 | -120.95 | | MAG/ANG |
| | -LD: | | .00 | .00 | | kW/kVR |
| kVll 24.900 | CAP: | | | .00 | | kVR |
| FROM NODE 808 |: | | .00 | .00 | | AMP/DG |
| <810 | > LOSS= | .002: | | (.002) | | kW |
| | * | A | * | B | * | C |
| NODE: 812 | VOLTS: | .976 | -1.57 | 1.010 | -121.92 | 1.007 118.59 MAG/ANG |
| | -LD: | .00 | .00 | .00 | .00 | .00 kW/kVR |
| kVll 24.900 | CAP: | | .00 | | .00 | .00 kVR |
| FROM NODE 808 |: | 51.95 -14.18 | 41.29 -127.99 | 39.33 116.90 AMP/DG | | |
| <812 | > LOSS= | 47.531: | (24.126) | (11.644) | (11.761) | kW |
| TO NODE 814 |: | 51.95 -14.18 | 41.29 -127.99 | 39.33 116.90 AMP/DG | | |
| <814 | > LOSS= | 37.790: | (19.245) | (9.140) | (9.404) | kW |
| | * | A | * | B | * | C |
| NODE: 814 | VOLTS: | .947 | -2.26 | .994 | -122.70 | .989 118.01 MAG/ANG |
| | -LD: | .00 | .00 | .00 | .00 | .00 kW/kVR |
| kVll 24.900 | CAP: | | .00 | | .00 | .00 kVR |
| FROM NODE 812 |: | 52.10 -14.73 | 41.29 -128.69 | 39.37 116.23 AMP/DG | | |
| <814 | > LOSS= | 37.790: | (19.245) | (9.140) | (9.404) | kW |
| TO NODE RG10 <VRG>.: |: | 52.10 -14.73 | 41.29 -128.69 | 39.37 116.23 AMP/DG | | |
| <RG10 | > LOSS= | .000: | (.000) | (.000) | (.000) | kW |
| | * | A | * | B | * | C |
| NODE: RG10 | VOLTS: | 1.018 | -2.26 | 1.026 | -122.70 | 1.020 118.01 MAG/ANG |
| | -LD: | .00 | .00 | .00 | .00 | .00 kW/kVR |
| kVll 24.900 | CAP: | | .00 | | .00 | .00 kVR |
| FROM NODE 814 <VRG>: | 48.47 -14.73 | 40.04 -128.69 | 38.17 116.23 AMP/DG | | | |
| <RG10 | > LOSS= | .000: | (.000) | (.000) | (.000) | kW |
| TO NODE 850 | : | 48.47 -14.73 | 40.04 -128.69 | 38.17 116.23 AMP/DG | | |
| <850 | > LOSS= | .017: | (.008) | (.005) | (.005) | kW |
| | * | A | * | B | * | C |
| NODE: 850 | VOLTS: | 1.018 | -2.26 | 1.026 | -122.70 | 1.020 118.01 MAG/ANG |
| | -LD: | .00 | .00 | .00 | .00 | .00 kW/kVR |
| kVll 24.900 | CAP: | | .00 | | .00 | .00 kVR |
| FROM NODE RG10 | : | 48.47 -14.73 | 40.04 -128.69 | 38.17 116.23 AMP/DG | | |
| <850 | > LOSS= | .017: | (.008) | (.005) | (.005) | kW |
| TO NODE 816 | : | 48.47 -14.73 | 40.04 -128.69 | 38.17 116.23 AMP/DG | | |
| <816 | > LOSS= | .538: | (.254) | (.145) | (.139) | kW |
| | * | A | * | B | * | C |

| | | | | | | | | |
|---------------|---------|----------|--------|----------|---------|----------|--------|---------|
| NODE: 816 | VOLTS: | 1.017 | -2.26 | 1.025 | -122.71 | 1.020 | 118.01 | MAG/ANG |
| | -LD: | .00 | .00 | .00 | .00 | .00 | .00 | kW/kVR |
| kVll 24.900 | CAP: | | .00 | | .00 | | .00 | kVR |
| <hr/> | | | | | | | | |
| FROM NODE 850 |: | 48.47 | -14.74 | 40.04 | -128.70 | 38.17 | 116.23 | AMP/DG |
| <816 > LOSS= | .538: | (.254) | | (.145) | | (.139) | | kW |
| TO NODE 818 |: | 13.02 | -26.69 | | | | | AMP/DG |
| <818 > LOSS= | .154: | (.154) | | | | | | kW |
| TO NODE 824 |: | 35.83 | -10.42 | 40.04 | -128.70 | 38.17 | 116.23 | AMP/DG |
| <824 > LOSS= | 14.181: | (4.312) | | (5.444) | | (4.425) | | kW |
| <hr/> | | | | | | | | |
| NODE: 818 | VOLTS: | 1.016 | -2.27 | | | | | MAG/ANG |
| | -LD: | .00 | .00 | | | | | kW/kVR |
| kVll 24.900 | CAP: | | .00 | | | | | kVR |
| <hr/> | | | | | | | | |
| FROM NODE 816 |: | 13.03 | -26.77 | | | | | AMP/DG |
| <818 > LOSS= | .154: | (.154) | | | | | | kW |
| TO NODE 820 |: | 13.03 | -26.77 | | | | | AMP/DG |
| <820 > LOSS= | 3.614: | (3.614) | | | | | | kW |
| <hr/> | | | | | | | | |
| NODE: 820 | VOLTS: | .993 | -2.32 | | | | | MAG/ANG |
| | -LD: | .00 | .00 | | | | | kW/kVR |
| kVll 24.900 | CAP: | | .00 | | | | | kVR |
| <hr/> | | | | | | | | |
| FROM NODE 818 |: | 10.62 | -28.98 | | | | | AMP/DG |
| <820 > LOSS= | 3.614: | (3.614) | | | | | | kW |
| TO NODE 822 |: | 10.62 | -28.98 | | | | | AMP/DG |
| <822 > LOSS= | .413: | (.413) | | | | | | kW |
| <hr/> | | | | | | | | |
| NODE: 822 | VOLTS: | .990 | -2.33 | | | | | MAG/ANG |
| | -LD: | .00 | .00 | | | | | kW/kVR |
| kVll 24.900 | CAP: | | .00 | | | | | kVR |
| <hr/> | | | | | | | | |
| FROM NODE 820 |: | .00 | .00 | | | | | AMP/DG |
| <822 > LOSS= | .413: | (.413) | | | | | | kW |
| <hr/> | | | | | | | | |
| NODE: 824 | VOLTS: | 1.008 | -2.37 | 1.016 | -122.94 | 1.012 | 117.76 | MAG/ANG |
| | -LD: | .00 | .00 | .00 | .00 | .00 | .00 | kW/kVR |
| kVll 24.900 | CAP: | | .00 | | .00 | | .00 | kVR |
| <hr/> | | | | | | | | |
| FROM NODE 816 |: | 35.87 | -10.70 | 39.82 | -129.02 | 38.05 | 116.25 | AMP/DG |
| <824 > LOSS= | 14.181: | (4.312) | | (5.444) | | (4.425) | | kW |
| TO NODE 826 |: | | | 3.10 | -148.92 | | | AMP/DG |
| <826 > LOSS= | .008: | | | (.008) | | | | kW |
| TO NODE 828 |: | 35.87 | -10.70 | 36.93 | -127.39 | 38.05 | 116.25 | AMP/DG |

| | | | | | | |
|-----------------------|--------------|---------------|---------------------|---------------------|---------------------|----------------------|
| <828 | > LOSS= | 1.108: | (.361) | (.393) | (.354) | kW |
| | * | | A | B | C | * |
| NODE: 826 | VOLTS: | | 1.016 | -122.94 | | MAG/ANG |
| | -LD: | | .00 | .00 | | kW/kVR |
| kVll 24.900 | CAP: | | | .00 | | kVR |
| FROM NODE 824 |: | | .00 | .00 | | AMP/DG |
| <826 | > LOSS= | .008: | | (.008) | | kW |
| | * | | A | B | C | * |
| NODE: 828 | VOLTS: | 1.007 | -2.38 | 1.015 | -122.95 | 1.011 117.75 MAG/ANG |
| | -LD: | .00 | .00 | .00 | .00 | .00 kW/kVR |
| kVll 24.900 | CAP: | | .00 | .00 | | .00 kVR |
| FROM NODE 824 |: | 35.87 -10.72 | 36.93 -127.41 | 37.77 116.42 AMP/DG | | |
| <828 | > LOSS= | 1.108: | (.361) | (.393) | (.354) | kW |
| TO NODE 830 |: | 35.87 -10.72 | 36.93 -127.41 | 37.77 116.42 AMP/DG | | |
| <830 | > LOSS= | 26.587: | (8.443) | (9.214) | (8.930) | kW |
| | * | A | B | C | * | |
| NODE: 830 | VOLTS: | .989 | -2.63 | .998 -123.39 | .994 117.25 MAG/ANG | |
| | D-LD: | 9.95 | 4.98 | 9.86 4.93 | 24.55 9.82 kW/kVR | |
| kVll 24.900 | Y CAP: | | .00 | .00 | | .00 kVR |
| FROM NODE 828 |: | 35.43 -11.06 | 36.91 -127.92 | 37.79 115.96 AMP/DG | | |
| <830 | > LOSS= | 26.587: | (8.443) | (9.214) | (8.930) | kW |
| TO NODE 854 |: | 34.22 -9.97 | 36.19 -127.47 | 36.49 116.26 AMP/DG | | |
| <854 | > LOSS= | .635: | (.197) | (.227) | (.211) | kW |
| | * | A | B | C | * | |
| NODE: 854 | VOLTS: | .989 | -2.64 | .998 -123.40 | .993 117.24 MAG/ANG | |
| | -LD: | .00 | .00 | .00 | .00 | .00 kW/kVR |
| kVll 24.900 | CAP: | | .00 | .00 | | .00 kVR |
| FROM NODE 830 |: | 34.23 -9.99 | 36.19 -127.48 | 36.49 116.25 AMP/DG | | |
| <854 | > LOSS= | .635: | (.197) | (.227) | (.211) | kW |
| TO NODE 852 |: | 34.23 -9.99 | 35.93 -127.72 | 36.49 116.25 AMP/DG | | |
| <852 | > LOSS= | 44.798: | (13.996) | (15.778) | (15.023) | kW |
| TO NODE 856 |: | | .31 -98.70 | | | AMP/DG |
| <856 | > LOSS= | .001: | | (.001) | | kW |
| | * | A | B | C | * | |
| NODE: 852 | VOLTS: | .958 | -3.11 | .968 -124.18 | .964 116.33 MAG/ANG | |
| | -LD: | .00 | .00 | .00 | .00 | .00 kW/kVR |
| kVll 24.900 | CAP: | | .00 | .00 | | .00 kVR |
| FROM NODE 854 |: | 34.35 -11.00 | 35.90 -128.66 | 36.52 115.41 AMP/DG | | |
| <852 | > LOSS= | 44.798: | (13.996) | (15.778) | (15.023) | kW |
| TO NODE RG11 .<VRG>.: | 34.35 -11.00 | 35.90 -128.66 | 36.52 115.41 AMP/DG | | | |

| <RG11 > LOSS= | | .000: | (.000) | (.000) | (.000) | kW | | |
|----------------|--------|--------|----------|----------|----------|-------|--------|----------|
| | | * | A | * | B | * | C | * |
| NODE: RG11 | VOLTS: | 1.036 | -3.11 | 1.035 | -124.18 | 1.036 | 116.33 | MAG/ANG |
| | -LD: | .00 | .00 | .00 | .00 | .00 | .00 | kW/kVR |
| kVll | 24.900 | CAP: | | .00 | | .00 | | .00 kVR |
| FROM NODE 852 | <VRG>: | 31.77 | -11.00 | 33.59 | -128.66 | 33.98 | 115.41 | AMP/DG |
| <RG11 > LOSS= | | .000: | (.000) | (.000) | (.000) | kW | | |
| TO NODE 832 |: | 31.77 | -11.00 | 33.59 | -128.66 | 33.98 | 115.41 | AMP/DG |
| <832 > LOSS= | | .011: | (.003) | (.004) | (.004) | kW | | |
| | | * | A | * | B | * | C | * |
| NODE: 832 | VOLTS: | 1.036 | -3.11 | 1.035 | -124.18 | 1.036 | 116.33 | MAG/ANG |
| | -LD: | .00 | .00 | .00 | .00 | .00 | .00 | kW/kVR |
| kVll | 24.900 | CAP: | | .00 | | .00 | | .00 kVR |
| FROM NODE RG11 |: | 31.77 | -11.00 | 33.59 | -128.66 | 33.98 | 115.41 | AMP/DG |
| <832 > LOSS= | | .011: | (.003) | (.004) | (.004) | kW | | |
| TO NODE 858 |: | 21.31 | .47 | 23.40 | -116.89 | 24.34 | 128.36 | AMP/DG |
| <858 > LOSS= | | 2.467: | (.643) | (.997) | (.827) | kW | | |
| TO NODE XF10 |: | 11.68 | -32.29 | 11.70 | -152.73 | 11.61 | 87.39 | AMP/DG < |
| <XF10 > LOSS= | | 9.625: | (3.196) | (3.241) | (3.187) | kW | | |
| | | * | A | * | B | * | C | * |
| NODE: 858 | VOLTS: | 1.034 | -3.17 | 1.032 | -124.28 | 1.034 | 116.22 | MAG/ANG |
| | -LD: | .00 | .00 | .00 | .00 | .00 | .00 | kW/kVR |
| kVll | 24.900 | CAP: | | .00 | | .00 | | .00 kVR |
| FROM NODE 832 |: | 20.86 | .86 | 23.13 | -116.39 | 24.02 | 128.48 | AMP/DG |
| <858 > LOSS= | | 2.467: | (.643) | (.997) | (.827) | kW | | |
| TO NODE 834 |: | 20.73 | 1.01 | 23.13 | -116.39 | 24.02 | 128.48 | AMP/DG |
| <834 > LOSS= | | 2.798: | (.717) | (1.145) | (.936) | kW | | |
| TO NODE 864 |: | .14 | -22.82 | | | | | AMP/DG |
| <864 > LOSS= | | .000: | (.000) | | | | | kW |
| | | * | A | * | B | * | C | * |
| NODE: 834 | VOLTS: | 1.031 | -3.24 | 1.029 | -124.39 | 1.031 | 116.09 | MAG/ANG |
| | -LD: | .00 | .00 | .00 | .00 | .00 | .00 | kW/kVR |
| kVll | 24.900 | CAP: | | .00 | | .00 | | .00 kVR |
| FROM NODE 858 |: | 20.29 | 2.18 | 22.37 | -116.07 | 23.23 | 130.06 | AMP/DG |
| <834 > LOSS= | | 2.798: | (.717) | (1.145) | (.936) | kW | | |
| TO NODE 842 |: | 14.75 | 34.68 | 16.30 | -95.63 | 15.12 | 151.05 | AMP/DG |
| <842 > LOSS= | | .064: | (.015) | (.032) | (.017) | kW | | |
| TO NODE 860 |: | 11.16 | -43.05 | 9.09 | -154.82 | 10.60 | 99.34 | AMP/DG |
| <860 > LOSS= | | .141: | (.021) | (.104) | (.017) | kW | | |
| | | * | A | * | B | * | C | * |
| NODE: 842 | VOLTS: | 1.031 | -3.25 | 1.029 | -124.39 | 1.031 | 116.09 | MAG/ANG |

| | | | | | | | | | |
|---------------|--------|----------|--------|---------|---------|----------|---------|---------|--------|
| | | -LD: | .00 | .00 | .00 | .00 | .00 | .00 | kW/kVR |
| kV11 | 24.900 | CAP: | | .00 | | .00 | | .00 | kVR |
| FROM NODE 834 |: | 14.74 | 34.67 | 16.30 | -95.64 | 15.12 | 151.03 | AMP/DG | |
| <842 > LOSS= | .064: | (.015) | | (.032) | | (.017) | | kW | |
| TO NODE 844 |: | 14.74 | 34.67 | 16.30 | -95.64 | 15.12 | 151.03 | AMP/DG | |
| <844 > LOSS= | .306: | (.068) | | (.156) | | (.083) | | kW | |
| | * | A | * | B | * | C | * | | |
| NODE: 844 | VOLTS: | 1.031 | -3.27 | 1.029 | -124.42 | 1.031 | 116.06 | MAG/ANG | |
| | Y-LD: | 143.41 | 111.54 | 142.97 | 111.20 | 143.51 | 111.62 | kW/kVR | |
| kV11 | 24.900 | Y CAP: | | 106.23 | | 105.90 | | 106.31 | kVR |
| FROM NODE 842 |: | 14.47 | 37.12 | 16.29 | -95.71 | 15.11 | 150.97 | AMP/DG | |
| <844 > LOSS= | .306: | (.068) | | (.156) | | (.083) | | kW | |
| TO NODE 846 |: | 9.83 | 78.88 | 9.40 | -63.87 | 9.40 | -170.67 | AMP/DG | |
| <846 > LOSS= | .323: | (.043) | | (.212) | | (.068) | | kW | |
| | * | A | * | B | * | C | * | | |
| NODE: 846 | VOLTS: | 1.031 | -3.32 | 1.029 | -124.46 | 1.031 | 116.01 | MAG/ANG | |
| | -LD: | .00 | .00 | .00 | .00 | .00 | .00 | kW/kVR | |
| kV11 | 24.900 | CAP: | | .00 | | .00 | | .00 | kVR |
| FROM NODE 844 |: | 9.76 | 78.80 | 9.40 | -52.54 | 9.78 | -161.93 | AMP/DG | |
| <846 > LOSS= | .323: | (.043) | | (.212) | | (.068) | | kW | |
| TO NODE 848 |: | 9.76 | 78.80 | 9.40 | -52.54 | 9.78 | -161.93 | AMP/DG | |
| <848 > LOSS= | .048: | (.007) | | (.031) | | (.010) | | kW | |
| | * | A | * | B | * | C | * | | |
| NODE: 848 | VOLTS: | 1.031 | -3.32 | 1.029 | -124.47 | 1.031 | 116.00 | MAG/ANG | |
| | D-LD: | 20.00 | 16.00 | 20.00 | 16.00 | 20.00 | 16.00 | kW/kVR | |
| kV11 | 24.900 | Y CAP: | | 159.43 | | 158.86 | | 159.56 | kVR |
| FROM NODE 846 |: | 9.76 | 78.79 | 9.77 | -42.47 | 9.78 | -161.94 | AMP/DG | |
| <848 > LOSS= | .048: | (.007) | | (.031) | | (.010) | | kW | |
| | * | A | * | B | * | C | * | | |
| NODE: 860 | VOLTS: | 1.030 | -3.24 | 1.029 | -124.39 | 1.031 | 116.09 | MAG/ANG | |
| | Y-LD: | 20.00 | 16.00 | 20.00 | 16.00 | 20.00 | 16.00 | kW/kVR | |
| kV11 | 24.900 | Y CAP: | | .00 | | .00 | | .00 | kVR |
| FROM NODE 834 |: | 5.87 | -33.62 | 7.68 | -156.52 | 5.29 | 86.10 | AMP/DG | |
| <860 > LOSS= | .141: | (.021) | | (.104) | | (.017) | | kW | |
| TO NODE 836 |: | 4.16 | -30.19 | 5.96 | -154.63 | 3.60 | 90.25 | AMP/DG | |
| <836 > LOSS= | .039: | (-.035) | | (.103) | | (-.028) | | kW | |
| | * | A | * | B | * | C | * | | |
| NODE: 836 | VOLTS: | 1.030 | -3.23 | 1.029 | -124.39 | 1.031 | 116.09 | MAG/ANG | |
| | -LD: | .00 | .00 | .00 | .00 | .00 | .00 | kW/kVR | |
| kV11 | 24.900 | CAP: | | .00 | | .00 | | .00 | kVR |

| | | | | | | | |
|---|----------|----------|----------|---------|-------|--------|----------|
| FROM NODE 860 | 1.49 | -19.83 | 4.42 | -150.74 | 1.74 | 68.08 | AMP/DG |
| <836 > LOSS= .039: | (-.035) | (.103) | (-.028) | kW | | | |
| TO NODE 840 | 1.50 | -20.01 | 2.33 | -151.97 | 1.75 | 68.00 | AMP/DG |
| <840 > LOSS= .002: | (-.014) | (.026) | (-.010) | kW | | | |
| TO NODE 862 | .00 | .00 | 2.09 | -149.38 | .00 | .00 | AMP/DG |
| <862 > LOSS= .000: | (-.005) | (.009) | (-.004) | kW | | | |
| ----- * ----- A ----- * ----- B ----- * ----- C ----- * | | | | | | | |
| NODE: 840 VOLTS: | 1.030 | -3.23 | 1.029 | -124.39 | 1.031 | 116.09 | MAG/ANG |
| Y-LD: | 9.27 | 7.21 | 9.26 | 7.20 | 9.28 | 7.22 | kW/kVR |
| kVll 24.900 Y CAP: | | .00 | | .00 | | .00 | kVR |
| ----- * ----- A ----- * ----- B ----- * ----- C ----- * | | | | | | | |
| FROM NODE 836 | .79 | -41.11 | .79 | -162.26 | .79 | 78.21 | AMP/DG |
| <840 > LOSS= .002: | (-.014) | (.026) | (-.010) | kW | | | |
| NODE: 862 VOLTS: | 1.030 | -3.23 | 1.029 | -124.39 | 1.031 | 116.09 | MAG/ANG |
| -LD: | .00 | .00 | .00 | .00 | .00 | .00 | kW/kVR |
| kVll 24.900 CAP: | | .00 | | .00 | | .00 | kVR |
| ----- * ----- A ----- * ----- B ----- * ----- C ----- * | | | | | | | |
| FROM NODE 836 | .00 | .00 | 2.09 | -149.50 | .00 | .00 | AMP/DG |
| <862 > LOSS= .000: | (-.005) | (.009) | (-.004) | kW | | | |
| TO NODE 838 | | | 2.09 | -149.50 | | | AMP/DG |
| <838 > LOSS= .004: | | | (.004) | | | | kW |
| ----- * ----- A ----- * ----- B ----- * ----- C ----- * | | | | | | | |
| NODE: 838 VOLTS: | | | 1.029 | -124.39 | | | MAG/ANG |
| -LD: | | | .00 | .00 | | | kW/kVR |
| kVll 24.900 CAP: | | | | .00 | | | kVR |
| ----- * ----- A ----- * ----- B ----- * ----- C ----- * | | | | | | | |
| FROM NODE 862 | | | .00 | .00 | | | AMP/DG |
| <838 > LOSS= .004: | | | (.004) | | | | kW |
| ----- * ----- A ----- * ----- B ----- * ----- C ----- * | | | | | | | |
| NODE: 864 VOLTS: | 1.034 | -3.17 | | | | | MAG/ANG |
| -LD: | .00 | .00 | | | | | kW/kVR |
| kVll 24.900 CAP: | | .00 | | | | | kVR |
| ----- * ----- A ----- * ----- B ----- * ----- C ----- * | | | | | | | |
| FROM NODE 858 | .00 | .00 | | | | | AMP/DG |
| <864 > LOSS= .000: | (.000) | | | | | | kW |
| ----- * ----- A ----- * ----- B ----- * ----- C ----- * | | | | | | | |
| NODE: XF10 VOLTS: | 1.000 | -4.63 | .998 | -125.73 | 1.000 | 114.82 | MAG/ANG |
| -LD: | .00 | .00 | .00 | .00 | .00 | .00 | kW/kVR |
| kVll 4.160 CAP: | | .00 | | .00 | | .00 | kVR |
| ----- * ----- A ----- * ----- B ----- * ----- C ----- * | | | | | | | |
| FROM NODE 832 | 69.90 | -32.29 | 70.04 | -152.73 | 69.50 | 87.39 | AMP/DG < |
| <XF10 > LOSS= 9.625: | (3.196) | (3.241) | (3.187) | kW | | | |
| TO NODE 888 | 69.90 | -32.29 | 70.04 | -152.73 | 69.50 | 87.39 | AMP/DG |

| <888 > LOSS= .000: | | (.000) | (.000) | (.000) | kW | | | |
|---------------------------|--------|-----------|---------|---------------|-----------|--------|---------|---|
| | | * | A | * | B | * | C | * |
| NODE: 888 | VOLTS: | 1.000 | -4.64 | .998 -125.73 | 1.000 | 114.82 | MAG/ANG | |
| | -LD: | .00 | .00 | .00 | .00 | .00 | kW/kVR | |
| kVll 4.160 | CAP: | | .00 | | .00 | | .00 kVR | |
| FROM NODE XF10: | | 69.90 | -32.29 | 70.04 -152.73 | 69.50 | 87.39 | AMP/DG | |
| <888 > LOSS= .000: | | (.000) | (.000) | (.000) | kW | | | |
| TO NODE 890: | | 69.90 | -32.29 | 70.04 -152.73 | 69.50 | 87.39 | AMP/DG | |
| <890 > LOSS= 32.760: | | (11.638) | | (9.950) | (11.173) | kW | | |
| | | * | A | * | B | * | C | * |
| NODE: 890 | VOLTS: | .917 | -5.19 | .924 -126.78 | .918 | 113.98 | MAG/ANG | |
| | D-LD: | 139.11 | 69.55 | 137.56 68.78 | 137.01 | 68.50 | kW/kVR | |
| kVll 4.160 | Y CAP: | | .00 | | .00 | | .00 kVR | |
| FROM NODE 888: | | 69.91 | -32.31 | 70.05 -152.75 | 69.51 | 87.37 | AMP/DG | |
| <890 > LOSS= 32.760: | | (11.638) | | (9.950) | (11.173) | kW | | |
| | | * | A | * | B | * | C | * |
| NODE: 856 | VOLTS: | | | .998 -123.41 | | | MAG/ANG | |
| | -LD: | | | .00 | .00 | | kW/kVR | |
| kVll 24.900 | CAP: | | | | .00 | | kVR | |
| FROM NODE 854: | | | | .00 | .00 | | AMP/DG | |
| <856 > LOSS= .001: | | | | (.001) | | | kW | |

The structure of 34-Node Test Feeder in Simulink

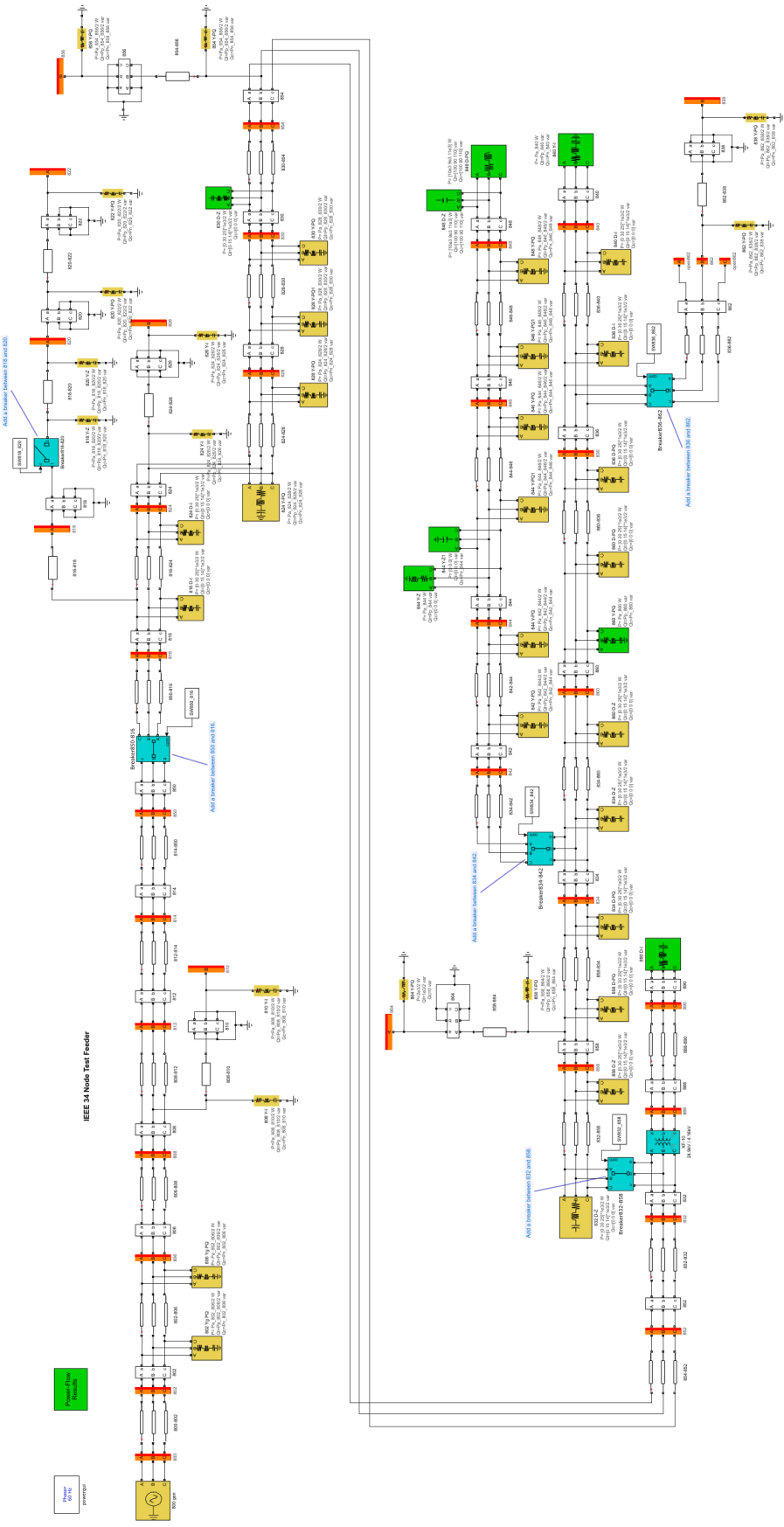


Figure 21: The structure of 34-Node Test Feeder in Simulink. [15]

Appendix B: Documented Computer Listings

The coding part of proposed neural network

```
#####
# building the model
input_image = Input(shape=(96, 96, 4))
### Downsampling ---- Encoder
print('-- Encoding --')
z = layers.Conv2D(16, (3,3), padding='same', activation='relu')(input_image) # shape 96 x 96
z = layers.BatchNormalization()(z)
z = layers.MaxPool2D((2,2))(z) # shape 48 x 48

z = layers.Conv2D(32, (3,3), padding='same')(z) # shape 48 x 48
z = layers.BatchNormalization()(z)
z = layers.MaxPool2D((2,2))(z) # shape 24 x 24
z = activations.relu(z)

z = layers.Conv2D(64, (3,3), padding='same', activation='relu')(z) # 24 x 24
z = layers.BatchNormalization()(z)
encoder = layers.MaxPool2D((2,2))(z) # shape 12 x 12

### Upsampling ---- Decoder
print('-- Decoding')
z = layers.Conv2D(64, (3, 3), padding='same', activation='relu')(encoder) # shape 12 x 12
z = layers.BatchNormalization()(z)
z = layers.UpSampling2D((2,2))(z) # shape 24 x 24

z = layers.Conv2D(32, (3, 3), padding='same')(z) # shape 24 x 24
z = layers.BatchNormalization()(z)
z = layers.UpSampling2D((2,2))(z) # shape 48 x 48
z = activations.relu(z)

z = layers.Conv2D(16, (3, 3), padding='same', activation='relu')(z) # shape 96 x 96
z = layers.BatchNormalization()(z)
z = layers.UpSampling2D((2,2))(z) # shape 48 x 48

# 4 channels because we have 4 channels in the input
decoder = layers.Conv2D(4, (3, 3), activation='sigmoid', padding='same')(z) # shape 48 x 48

# Building the model
autoencoder = Model(input_image, decoder)

# Printing the model summary
print(autoencoder.summary())
#####
```

Figure 22: Autoencoder Code for all Models